

*Digital Comprehensive Summaries of Uppsala Dissertations  
from the Faculty of Medicine 2114*

# Inter-organelle crosstalk in the pancreatic $\beta$ cell: Membrane contact sites as regulators of insulin secretion

STYLIANI PANAGIOTOU



ACTA UNIVERSITATIS  
UPSALIENSIS  
2025

ISSN 1651-6206  
ISBN 978-91-513-2339-8  
urn:nbn:se:uu:diva-544607



UPPSALA  
UNIVERSITET

Dissertation presented at Uppsala University to be publicly examined in A1:107a, Biomedical Center, Husargatan 3, Uppsala, Friday, 14 February 2025 at 13:15 for the degree of Doctor of Philosophy (Faculty of Medicine). The examination will be conducted in English. Faculty examiner: Associate Professor Samuel Stephens (University of Iowa).

### **Abstract**

Panagiotou, S. 2025. Inter-organelle crosstalk in the pancreatic  $\beta$  cell: Membrane contact sites as regulators of insulin secretion. *Digital Comprehensive Summaries of Uppsala Dissertations from the Faculty of Medicine* 2114. 72 pp. Uppsala: Acta Universitatis Upsaliensis. ISBN 978-91-513-2339-8.

Pancreatic  $\beta$  cells play a crucial role in glucose homeostasis by producing and secreting insulin. Impaired insulin release leads to chronic hyperglycemia and contributes to the development of type 2 diabetes (T2D). Insulin is stored in secretory granules, which are transported to the plasma membrane for exocytosis to the circulation in response to elevated blood glucose levels. The mechanisms that couple glucose metabolism to insulin secretion are complex and involve both  $\text{Ca}^{2+}$  and phospholipid signaling. Membrane contact sites (MCSs) are specialized regions where organelle membranes are closely apposed, providing a conduit for non-vesicular lipid exchange and  $\text{Ca}^{2+}$  transport between the two compartments, but their importance for normal  $\beta$  cell function is not known. Here, we discover a new type of MCS involving the ER and insulin granules, which facilitate lipid exchange between the two organelles. Oxysterol-binding protein (OSBP), a cytosolic lipid transport protein (LTP), was recruited to these MCSs in a  $\text{Ca}^{2+}$ - and pH-dependent manner and catalyzed the exchange of granular PI(4)P for ER cholesterol. This mechanism was essential for normal insulin secretion. Transmembrane protein 24 (TMEM24) is an ER-anchored LTP that dynamically interacts with the plasma membrane (PM) and provides it with phosphatidylinositol, a precursor of other phosphoinositides. We found that TMEM24 localization was spatially and temporally regulated by  $\text{Ca}^{2+}$  and diacylglycerol (DAG), and that, upon dissociation from the PM, it stabilized at ER-mitochondria MCSs. Loss of TMEM24 led to dysregulation of both ER and mitochondria  $\text{Ca}^{2+}$ , impaired ATP production, and reduced insulin secretion. High-resolution imaging further revealed that TMEM24 also localized close to a subset of newly synthesized insulin granules that were in proximity to mitochondria. These organelle contacts were additionally defined by the presence of voltage-dependent anion channel (VDAC) and Mitofusin-2 on the mitochondria and the vesicular nucleotide transporter (VNUT) on the insulin granules. Reduced VNUT expression abolished the interaction between mitochondria and insulin granules and led to impaired insulin granule biogenesis and exocytosis. Collectively, our findings highlight the significant roles of different MCSs in maintaining normal  $\beta$  cell function.

*Keywords:* Membrane Contact Sites, Phosphoinositides,  $\text{Ca}^{2+}$ , Lipid Transport Proteins, Endoplasmic Reticulum, Insulin Secretory Granules, Mitochondria, ATP, Insulin Secretion

*Styliani Panagiotou, Department of Medical Cell Biology, Box 571, Uppsala University, SE-75123 Uppsala, Sweden.*

© Styliani Panagiotou 2025

ISSN 1651-6206

ISBN 978-91-513-2339-8

URN urn:nbn:se:uu:diva-544607 (<http://urn.kb.se/resolve?urn=urn:nbn:se:uu:diva-544607>)

“All things are mutually woven together and therefore have an affinity for each other”

Marcus Aurelius, *Meditations*.

To my family



# List of Papers

This thesis is based on the following papers, which are referred to in the text by their Roman numerals.

- I. Xie, B., **Panagiotou, S.**, Cen, J., Gilon, P., Bergsten, P., & Idevall-Hagren, O. (2021) The endoplasmic reticulum–plasma membrane tethering protein TMEM24 is a regulator of cellular Ca<sup>2+</sup> homeostasis. *Journal of Cell Science*, 135(5)
- II. **Panagiotou, S.**, Tan, K. W., Nguyen, P. M., Müller, A., Oqua, A. I., Tomas, A., Wendt, A., Eliasson, L., Tengholm, A., Solimena, M., & Idevall-Hagren, O. (2024) OSBP-mediated PI(4)P-cholesterol exchange at endoplasmic reticulum-secretory granule contact sites controls insulin secretion. *Cell Reports*, 43(4), 113992
- III. **Panagiotou, S.** and Idevall-Hagren, O. (2024) Organelle cross-talk controls the early stages of insulin granule maturation. (*manuscript*)

Reprints were made with permission from the respective publishers.



# Contents

Introduction .....	11
The pancreatic islets of Langerhans .....	11
Diabetes .....	11
Insulin biogenesis and exocytosis.....	12
Glucose-stimulated insulin secretion .....	13
Insulin granule subpopulations.....	14
Vesicular ATP uptake and storage.....	16
Mitochondrial dynamics in $\beta$ cells.....	17
Membrane Contact sites .....	18
Membrane contact sites in $\beta$ cells .....	20
Membrane contact sites- associated diseases.....	21
Membrane contact sites and type-2 diabetes .....	22
Phosphoinositides .....	23
Phosphatidylinositol-4-phosphate (PI[4]P).....	24
The role of phosphoinositides in MCS formation.....	25
Cholesterol biosynthesis and function in $\beta$ cells .....	26
Aims .....	28
Methodology .....	29
Pancreatic $\beta$ -cell models.....	29
Live cell imaging .....	30
Ca <sup>2+</sup> imaging techniques and indicators .....	31
Insulin secretion measurement <i>in vitro</i> .....	32
Visualization of membrane contact sites .....	33
Visualization of cholesterol .....	35
Results and discussion.....	36
Paper I.....	36
Distribution of TMEM24 is controlled by DAG and Ca <sup>2+</sup> .....	37
TMEM24 supports sustained insulin secretion and regulate ER Ca <sup>2+</sup> .....	37
TMEM24 regulates mitochondrial Ca <sup>2+</sup> homeostasis and ATP production.....	38

Paper II .....	40
Detection of contact sites between the ER and the ISGs .....	40
OSBP localizes to ER-ISG contact sites in a PI(4)P-dependent manner .....	41
OSBP binding to ISGs is regulated by Ca <sup>2+</sup> and cytosolic pH .....	42
Coordination of OSBP and Sac2 on the surface of ISGs controls insulin secretion .....	43
Paper III .....	45
TMEM24 is recruited to newly synthesized insulin granules.....	45
Time-dependent interactions between mitochondria and newly synthesized ISGs .....	46
Colocalization between VNUT and VDAC at newly synthesized ISGs .....	46
Reduced VNUT expression affects VDAC localization to newly synthesized ISGs and impairs ISG maturation.....	47
Reduced VNUT expression impairs insulin secretion .....	48
Conclusions .....	49
Future Perspectives .....	50
Περίληψη.....	53
Acknowledgements .....	56
References .....	59



# Abbreviations

ATP	Adenosine triphosphate
CPA	Cyclopiazonic acid
DAG	Diacylglycerol
ddRFP	Dimerization-dependent Red Fluorescent Protein
ER	Endoplasmic reticulum
FM	Fluorescence microscopy
FFAT	Two phenylalanine in an acidic tract
FP	Fluorescent protein
GECI	Genetically encoded calcium indicators
GFP	Green fluorescent protein
ISG	Insulin secretory granule
MCS	Membrane contact site
Mfn2	Mitofusin 2
OSBP	Oxysterol-binding protein
PA	Phosphatidic acid
PAO	Phenylarsine oxide
PH	Pleckstrin homology
PI	Phosphoinositide
PI(4)P	Phosphatidylinositol 4-phosphate
PI(4,5)P <sub>2</sub>	Phosphatidylinositol 4,5-bisphosphate
PKC	Protein kinase C
PLC	Phospholipase C
PM	Plasma membrane
RRP	Readily releasable pool
RUSH	Retention Using Selective Hooks
SDCM	Spinning disk confocal microscopy
SERCA	Sarco/endoplasmic reticulum Ca <sup>2+</sup> -ATPase
SNARE	Soluble NSF attachment protein receptor
T2D	Type 2 diabetes
TIRF	Total internal reflection fluorescence
VAP-A	VAMP-associated protein A
VDAC	Voltage-dependent anion channel
VDCC	Voltage-dependent calcium channel
VNUT	Vesicular Nucleotide Transporter



# Introduction

## The pancreatic islets of Langerhans

The pancreatic islets of Langerhans occupy 1-2% of the total pancreas volume [1]. They harbour their own vasculature receiving up to 20% of the total pancreatic blood supply. Each one of them contains approximately 2,000 hormone-producing cells. The endocrine cells are classified based on the type of hormone they release. A pancreatic islet consists of  $\beta$  cells (insulin and islet amyloid polypeptide),  $\alpha$  cells (glucagon),  $\delta$  cells (somatostatin),  $\gamma$  cells (pancreatic polypeptide cells) and rare  $\epsilon$  cells (ghrelin).  $\beta$  cells are the most abundant, corresponding to 65-80% of the endocrine cells in rodent islets [1, 2]. The hormone secretion by the islets of Langerhans is controlled by metabolic, endocrine and paracrine regulatory mechanisms and they are essential for the regulation of metabolic fuel homeostasis. Insulin secretion is stimulated by glucose uptake and, in turn, it suppresses the hepatic glucose output and adipose tissue lipolysis, while it stimulates glucose uptake into fat and the muscle cells. It also inhibits endogenous glucose production, primarily in the liver [3]. Glucagon has a counteracting effect, preventing the drop of blood glucose and the development of hypoglycaemia by stimulating glucose production in the liver cells and fatty acid secretion from the adipose tissue [4]. Somatostatin secretion suppresses both glucagon and insulin release [5, 6]. Given that glucose is the main energy source for the brain and the nervous system, the maintenance of glucose homeostasis by the proper function of the pancreatic islets is essential.

## Diabetes

Insulin deficiency due to the destruction of pancreatic  $\beta$  cells leads to type 1 diabetes (T1D). The onset is usually during childhood or adolescence and even though the etiology is not fully identified, it involves islet-targeting autoantibodies, resulting in  $\beta$ -cell damage, disruption of insulin synthesis and secretion, and thus hyperglycemia [7]. The pathogenesis of type 2 diabetes (T2D) is more complicated and is characterized by high blood glucose concentration (hyperglycemia) and altered lipid metabolism caused by the failure of the peripheral tissues to respond to insulin (insulin resistance) which forces the  $\beta$  cells to secrete higher amounts of insulin (hyperinsulinemia) that eventually lead to islet dysfunction [8, 9]. Insulin resistance is related to genetic factors

as well the prevalence of obesity [7, 10]. In addition to genetic predisposition, the sedentary lifestyle coupled with the excessive food consumption are leading causal factors for obesity which increases the risk of many chronic diseases, including type 2 diabetes. Another hypothesis posits that the visceral adiposity drives the lipid overflow to the peripheral tissues increasing the risk of T2D. Along with the increasing levels of ectopic lipid infiltration, elevated levels of circulating free-fatty acids can also result in a condition known as 'lipotoxicity', causing direct oxidative stress in the islets cells [11]. Even though it is not fully understood which is the leading cause of T2D, disruptions in the insulin secretory pathway in  $\beta$  cells have been observed both in diabetes models and human pancreatic islets from patients with T2D. Defects in calcium signaling, insulin biogenesis and insulin granule exocytosis contributes to the loss of normal glucose-stimulated insulin secretion in T2D [12].

## Insulin biogenesis and exocytosis

A  $\beta$  cell contains approximately 10,000 insulin granules that make up 5-10% of the total protein content of the cell [13, 14]. Insulin synthesis starts with the translation of preproinsulin mRNA where the signal peptide guides the ribosome to the ER, facilitating preproinsulin translocation across the ER membrane and into the lumen, where it is eventually cleaved [15, 16]. Proinsulin molecules are stabilized due to the activity of chaperone proteins (GRP94) and the interaction with zinc ions [17]. They consist of an A chain and a B chain, connected with a peptide segment of about 30 residues, and a C chain. Upon further modifications by Golgi-localized enzymes, proinsulin, together with calcium and zinc ions, is packed into vesicles that bud off from the TGN. This Golgi origin leads to high concentration of phosphatidylinositol 4-phosphatase (PI[4]P) in the granule membrane, which is maintained by the presence of ISG-localized PI4-kinases [18]. In addition to that, insulin secretory granules (ISGs) have high membrane cholesterol content due to the activity of the oxysterol-binding proteins (OSBP) [19, 20] and the ATP-binding cassette (ABC)-type of cholesterol transporters [21]. However, these immature insulin granules must undergo multiple maturation steps during which the original lipid and protein composition change, before they fuse with the plasma membrane. During the maturation process, the pH in the granular lumen drops due to the activity of ATP-dependent  $H^+$ -pumps and the C chain is removed from proinsulin, generating insulin [22, 23].

Prior to insulin release, there is a series of well-orchestrated processes which regulate exocytosis. Cytoskeleton remodelling is essential for insulin secretion from  $\beta$  cells, as the actin filaments and the microtubule network (MT) regulate the transport of ISGs from the cell periphery to the plasma membrane. The transport of ISGs begins with long-distance movement along microtubules (MTs), driven by kinesin motors [24, 25]. This is followed by a

transfer to myosin V, which facilitates short-range movement along actin filaments toward the plasma membrane [24, 25]. Under basal conditions, the actin filaments and MTs act as barriers to block the transport and release of ISGs, whereas, upon glucose stimulation the cytoskeleton depolymerizes to facilitate the insulin secretion [24, 25]. Small GTPases of the Rab family, including Rab3, support the tethering of insulin granules to the plasma membrane, a process called docking [26]. After the interaction of Rab3 $\alpha$  with RIM2 $\alpha$ , the proteins of the SNARE complex, syntaxin-1 and Munc18, are recruited at the docking sites to secure the immobilization of the vesicles. After docking, not all granules will necessarily fuse with the plasma membrane. The granules that will succeed, undergo first the priming step [27, 28]. This process, even though not fully understood, includes conformational changes of the SNARE complex and requires energy consumption [14, 29]. Some of the proteins involved in this machinery are CAPS (Ca<sup>2+</sup>-dependent activator protein in secretion) [30], Munc-13 [31, 32], and Doc2b [33] and involves the recruitment of the L-type voltage-dependent Ca<sup>2+</sup> channels (VDCCs) [34]. SNAP-25, VAMP-2 and plasma membrane Syntaxin-1a [32] support the final fusion step of the granules with the plasma membrane. These preferentially occur in proximity to sites of Ca<sup>2+</sup> influx through VDCCs [34].

## Glucose-stimulated insulin secretion

Mature insulin granules are classified into two groups. Of the 10,000 insulin granules, 75-95% of them correspond to the reserve pool which is located at distance from the plasma membrane. The rest of insulin is stored in a small fraction of granules that are localized close to the plasma membrane, called the readily releasable pool (RRP) [35]. Glucose stimulates insulin secretion from  $\beta$  cells in a bi-modal fashion. During the first phase, which lasts 5-10 min, the RRP releases its content at a rate of 20 insulin granules/min. The second phase is prolonged and sustain insulin secretion at a lower rate of 6 granules/min, as it involves mobilization of granules from the reserve pool and trafficking along microtubules to the plasma membrane [35, 36].

Other nutrients, besides glucose, can stimulate insulin secretion, such as certain amino acids [37], fatty acids [38] and neurotransmitters [39]. Glucose enters the  $\beta$  cell through the GLUT transporters (GLUT1 in humans and GLUT2 in mice). It quickly undergoes glycolysis where it first gets phosphorylated to glucose-6-phosphatase and, upon a sequence of reactions, pyruvate is generated which oxidizes to Acetyl CoA. This final product of glycolysis enters the mitochondria and is fed into the Krebs cycle with subsequent oxidative phosphorylation. This causes an increase in the ATP/ADP ratio in the cytosol. As a result, the ATP-sensitive K<sup>+</sup> channels in the plasma membrane close, preventing the K<sup>+</sup> extrusion and leading to membrane depolarization. The activation of pyruvate kinase (PK), which converts ADP and phosphoenolpyruvate (PEP) into ATP and pyruvate can independently contribute to the

elevation of ATP/ADP leading to the  $K_{ATP}$ -channel closure [40]. At a certain membrane potential the VDCCs open, inducing a rise of the cytosolic  $Ca^{2+}$  concentration which triggers insulin granule exocytosis (Figure 1) [41].

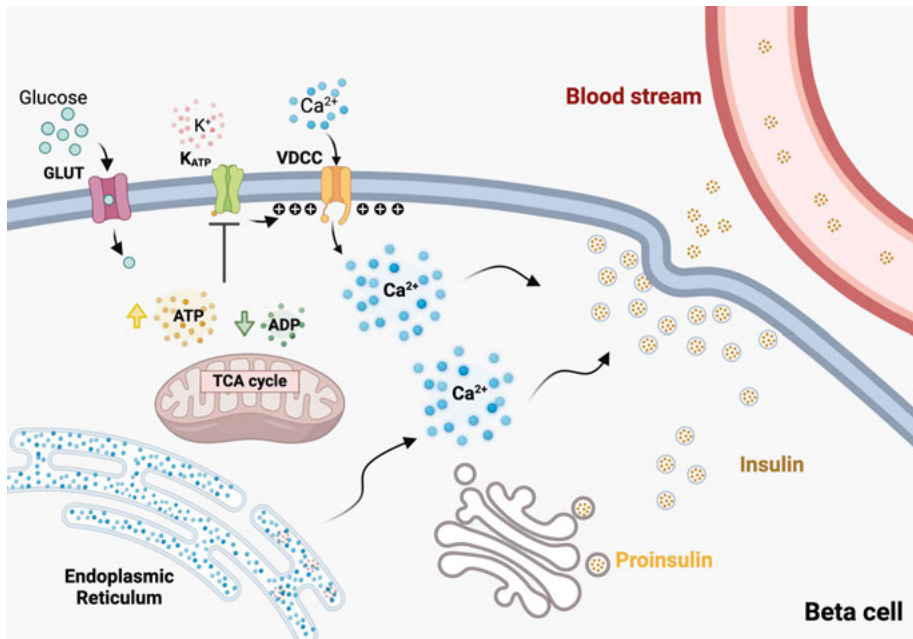


Figure 1: Glucose-stimulated insulin secretion

## Insulin granule subpopulations

Within  $\beta$  cells, the storage, processing and trafficking of insulin occur inside the insulin secretory granules (ISGs). The ISG exocytosis is coordinated by the activation of the cellular machineries localized on both the plasma membrane and the ISGs (Figure 2) [42]. Upon glucose stimulation, only 1-2% of the total ISG content is released indicating that various spatiotemporal variables define the release competence of the insulin granules [35]. The ISG selection for secretion in the  $\beta$  cell is a well-researched but not well-understood process. The distance of ISG from the plasma membrane [35] and the docking efficiency [35, 43] are important determinants of the ISG secretory capacity. Insulin granules positioned close to the plasma membrane and/or in physical interaction with the soluble N-ethylmaleimide-sensitive factor attachment protein receptor (SNARE) complex constitute the readily-releasable pool which contributes to the first-phase insulin secretion that occurs within seconds of depolarization [12, 44-46]. However, plasma membrane proximity is not a prerequisite for ISG fusion [47]. The ISG propensity for translocation to the plasma membrane can be affected by the ISG mobility [48] and age [48-

50]. ISGs with high mobility can be rapidly transported from the inner cytoplasmic space to the plasma membrane, traveling on the microtubule network, and undergo exocytosis upon glucose-induced  $\text{Ca}^{2+}$  influx [51, 52]. In addition to their mobility, ISG age plays an important role, with newly synthesized ISGs having a greater propensity for exocytosis compared with older ones [24, 49, 53, 54] as it was reported as early as 1987. Using radiolabelled pancreatic slices it was demonstrated that insulin synthesized within the last 3 h was preferentially released over older insulin [55]. In the 2000s, the development of “fluorescent timer proteins” confirmed the age-dependent segregation of ISGs in distinct populations [56, 57] and in 2012 Hou et al., using HaloTag-based multi-labelling reporter system coupled with pulse-chase methodology, verified the preferential release of newly synthesized ISGs in the pancreatic  $\beta$  cell line, MIN6 [58]. The proteomic and lipidomic characterization of age-distinct ISG pools has been the main focus of various studies [50, 59-61]. However, the flow cytometry-based identification processes have been hampered by the technical limitations during the ISG isolation protocols due to cross-contamination by other subcellular compartments with similar physical properties, such as lysosomes and endosomes. The most commonly used organelle purification protocols, based on subcellular fractionation, either by differential or gradient centrifugation, resulted in the co-enrichment of non-ISG proteins, while several well-established ISG transmembrane and cargo proteins are not detected [62]. Recent efforts have focused on the organelle immunoisolation using antibodies against the cytoplasmic domain of the target proteins [63-65]. However, inevitable contamination is observed by post-Golgi apparatus vesicle transmembrane proteins. Taking advantage of the specificity of the immunoprecipitation, Neukam and coworkers used the cleavable CLIP tag in combination with pulse-chase labelling allowing the purification of intact ISG from age-distinct pools in INS-1 cells. The study revealed changes in the ISG lipid composition over time highlighting that the ratio of phosphatidylcholine to phosphatidylethanolamine alters the physical properties of the ISG membrane, affecting the fluidity and charge of ISG membranes *in vitro* indicating an MCS-mediated mechanism for lipid transfer on the ISGs rather than a direct enzymatically-catalysed lipid exchange. Interestingly, according to their results, there is differential enrichment of the kinesin-1 heavy chain (KIF5b) as well as the Ras-related protein 3a (RAB3a) as these proteins associate preferentially with the younger granules [66].

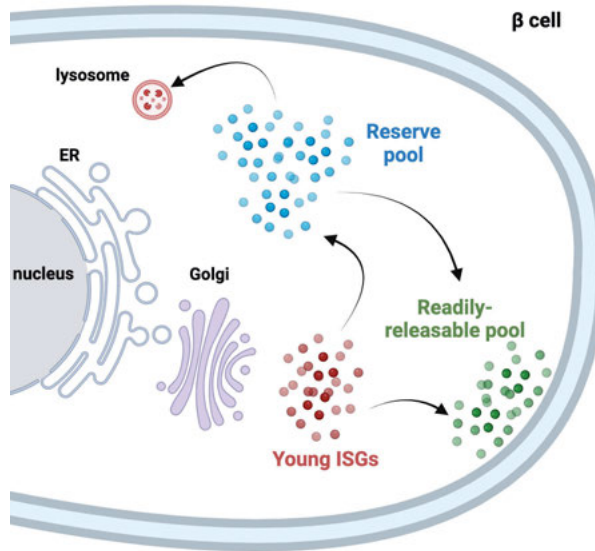


Figure 2: Insulin granule population consists of a “readily-releasable pool” of ISG of localised to the  $\beta$ -cell plasma membrane and the “reserve pool” which is deeper in the cytosol.

### Vesicular ATP uptake and storage

ATP is broadly known as a major form of molecular energy currency, providing energy for a plethora of intracellular biological processes. Although ATP-release from the nerves [67] was observed in the late 1950s and the purinergic transmission was described in the 1972 [68], the contribution of vesicular ATP in the mechanism rose various concerns regarding its role as an extracellular signalling molecule as it was still unclear how it entered into the secretory organelles that underwent exocytosis [67]. ATP release can be the result of exocytosis, channel-mediated release (pannexin) and cell breakdown [69-72]. In the extracellular space, ATP is hydrolysed to ADP and adenosine. ATP, ADP and UTP can bind to their respective purine receptors stimulating a variety of signalling cascades including inflammation, neurological interactions and mechanical transductions [72]. The purinoreceptors are classified into two groups; the G-coupled receptors (GPCRs), P2Y, which are stimulated by ATP, UTP and adenosine and the ligand-gated channels, P2X receptors, which produce ATP-dependent cation currents [73]. Upon binding to the purinergic receptors, ATP and the products of its hydrolysis trigger a positive feedback signal amplifying glucose-induced insulin release. Moreover, external ATP is a key element of insulin secretion pulsatility and can entrain  $\beta$  cells to exhibit coordinated  $\text{Ca}^{2+}$  oscillations [74-76]. Vesicular ATP accumulation was first described in the chromaffin granules in 1978 [77, 78]. However, the exact



mechanism of the ATP transport remained unelucidated for decades. SLC17 is a type I phosphate transporter family consisting of four subfamilies: SLC17A1–4, SLC17A5, SLC17A6–8 and SLC17A9 [79]. In 2008, Moriyama and colleagues [80] showed that the SLC17A9 gene encoded the vesicular nucleotide transporter (VNUT), an ATP transporter which was highly expressed in the adrenal gland, the cerebral cortex, the olfactory bulb, the hippocampus and the thyroid gland [80, 81]. This discovery revealed the molecular mechanism behind the vesicular ATP uptake and storage that could allow the initiation of the purinergic chemical transmission in ATP-secreting cells [72]. The SLC17A9 gene is located on chromosome 20 and consist of 14 exons and 13 introns [72]. VNUT comprises 12 putative transmembrane regions, with very short amino- and carboxy- terminal regions facing the cytoplasm [72, 82]. The electrochemical gradient of  $H^+$  across the vesicular membrane, and more specifically the membrane potential, in combination with the presence of millimolar concentration of  $Cl^-$ , serves as the driving force for VNUT-mediated transport of nucleotides in the lumen of the vesicles in neurons and chromaffin cells [72].

Immunohistochemical labelling and immunoelectron microscopy studies showed that  $\alpha$ - and  $\beta$ -, but not  $\delta$ -cells, along with acinar cells expressed VNUT [83]. In  $\beta$  cells, VNUT was associated with insulin granules. Insulin and ATP secretion was significantly reduced upon glucose-stimulation in VNUT<sup>-/-</sup> mice compared to the wild-type, indicating that ATP and insulin are co-stored and co-secreted under high glucose conditions via a VNUT-dependent mechanism [83]. Notably, no apparent morphological changes were observed in insulin granules in VNUT<sup>-/-</sup> mice. However, methodological differences between studies on VNUT have led to contradictory conclusions. Studies from Geisler et al. in isolated islets and MIN6 cells revealed that ATP enhances insulin secretion through activation of the P2Y receptor signalling [84]. On the other hand, the islets of VNUT<sup>-/-</sup> mice exhibited impaired ATP release but enhanced insulin secretion upon glucose stimulation [83]. These results indicate the involvement of ATP in negative feedback regulation of insulin release *in vivo*, potentially explained by the predominant presence of purinoreceptors with inhibitory effect compared to purinoreceptors with stimulatory effect on insulin secretion or by the VNUT deletion in alpha cells [83]. Interestingly, VNUT<sup>-/-</sup> mice were hypoglycaemic during glucose tolerance test indicating increased glucose sensitivity which suggests that VNUT is a potential and novel therapeutic target in diabetes research [83].

## Mitochondrial dynamics in $\beta$ cells

Mitochondria are organelles comprising an inner and an outer membrane separated by the intermembrane space. Mitochondria exist as a dynamic reticular network that frequently undergoes regulated fission and fusion cycles, referred

to as “mitochondrial dynamics”, which promotes their optimal function [85]. Mitochondrial fusion is the physical merging of the outer and inner mitochondrial membranes of two originally distinct mitochondria, and is a mechanism that can compensate for damaged and dysfunctional mitochondria. Fission, on the other hand, corresponds to the mitochondrial division which is responsible for the removal of damaged or non-functional mitochondria through mitophagy as well as the inheritance and partitioning of organelles during cell division [86]. In  $\beta$  cells, around 80% of glucose oxidation takes place in mitochondria [87]. From the sequence of events, described in a previous section, it is evident that mitochondria of  $\beta$  cells control glucose-stimulated insulin secretion, in particular by transferring the stored energy of glucose, the chief stimulator of insulin secretion, to ATP, triggering exocytosis. Therefore, disturbances in the tuning of the mitochondrial fusion/fission process in the pancreatic  $\beta$  cell are responsible for the development or/and the progression of diabetes [88]. In turn, chronic exposure to high glucose levels or fatty acids during diabetes leads to increased production of reactive oxygen species (ROS), mitochondrial dysfunction and enhanced cell apoptosis [89-91].  $\beta$  cells in pancreatic islets obtained from patients with T2D demonstrated functional and structural abnormalities, including reduced ATP levels, lower number of insulin granules, with a consequent decrease in insulin secretion [92, 93]. Altered expression of the proteins involved in the mitochondrial fusion/fission machineries has a critical role in perpetuating diabetes and its complications [88]. Mice with  $\beta$  cell-specific knockout of Mitofusin1/2, the main contributors of mitochondrial fusion, displayed higher degree of fragmented mitochondria and disrupted cristae structure as well as glucose intolerance and impaired insulin secretion due to loss of mtDNA content [94]. On the other hand, the mitochondrial fragmentation is mainly mediated by dynamin-related protein 1 (Drp1), which together with the mitochondrial fission factor (Mff) and fission protein 1 (Fis1) can cause conformational changes and induce mitochondrial fission [95]. Genetic or pharmacologic inhibition of Drp1 impaired ATP-associated respiration and increased proton leak resulting in reduces insulin secretion [96, 97]. However, the regulators of mitochondrial dynamics are involved in multifaceted molecular mechanisms which hampers the development of a therapeutic strategy targeting them.

## Membrane Contact sites

Cellular compartments do not act as separate units and can be actively positioned very close to each other forming specialized cellular regions [98-100]. Membrane contact sites (MCSs) have recently received growing interest as it has become clear that they significantly contribute to cellular responses to environmental and developmental changes. The tight inter-organelle coordination acts as a hotspot for communication and material transfer. Some of the

functions that occur in the MCSs include the exchange of signals and metabolites (calcium, ROS, lipids) that in turn regulate processes such as autophagy, lipid metabolism, organelle trafficking, apoptosis and membrane dynamics. This physical interaction can affect either or both organelles involved. The distance between the two membranes and the stability of the contacts can exhibit a considerable variability. In mammalian cells, this distance is usually 10-20 nm [101] and can last from 1 second up to the lifetime of the cell, as in the muscle tissue [102, 103]. The MCS composition affects the function of the MCS, and two organelles can form more than one type of MCS.

ER is the largest membrane-bound organelle in the eukaryotic cells, consisting of flat membrane cisternae (also known as sheets), covered with ribosomes, and tubules, branched and spread throughout the cytosol [104, 105]. MCSs are remarkably extensive along the tubular ER membrane. The ER forms MCSs with mitochondria, endosomes, Golgi, peroxisomes, lipid droplets and the plasma membrane (Figure 3). At these MCSs, the organelles are closely opposed but not fused, containing highly specialized molecular machineries that regulate essential cellular process, including lipid and ion exchange, organelle division and distribution. Although for many years MCSs were considered short-lived interactions, established for the quick material transfer, the advent of improved spatial and temporal resolution microscopy revealed that other organelles can remain tightly tethered to the ER during their trafficking [100].

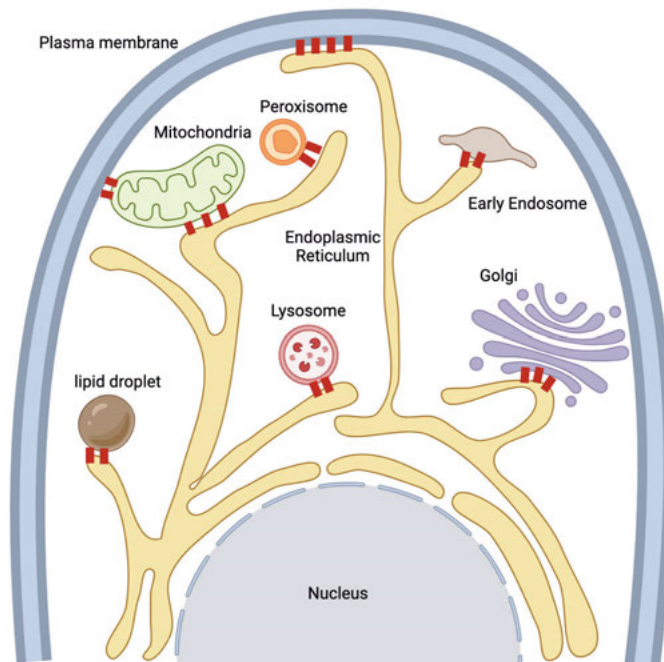


Figure 3: ER membrane contact sites with other organelles and the plasma membrane.

Organelle proximity is necessary but not sufficient to form MCSs. Several criteria should be met. First, the organelle integrity should be maintained and the membrane fusion should be avoided [106]. MCSs are identified by active tethering which is mediated by protein complexes attached to the surface of the interacting organelles [106]. Besides the tethering molecules, MCSs have a distinct molecular composition with specialized proteome [107, 108] which defines the biological function of the MCS. One important function of organelle proximity is to facilitate intracellular lipid trafficking. Lipid transport proteins (LTPs) mediate the non-vesicular transfer of phospholipids, sterols, ceramides and fatty acids [109]. Their hydrophobic cavity can extract and transfer the lipidic molecule, while their transmembrane domain or motifs that interact with ER-anchored vesicle-associated membrane proteins (VAMP)-associated protein (VAPs) can be used to stabilize it between the tethered membranes [109]. In our study, we focus on lipid transport mediated by the oxysterol-binding protein (OSBP), which is involved in the formation of contacts between the ER and the TGN. OSBP binds the ER-localized VAP via an acidic tract (FFAT) motif [110-113] and the Golgi membrane via the pleckstrin homology (PH) domain-dependent PI(4)P interactions [114, 115]. The PI(4)P gradient between the two membranes serves as the driving force for OSBP to transport cholesterol to the Golgi and PI(4)P in the opposite direction, both through the ORD domain [116]. Similar counter-transfer of lipid cargo has also been described for the ER-anchored ORP5 and ORP8 that, through binding to PI(4)P and PI(4,5)P<sub>2</sub> on the PM, transport phosphatidylserine from the PM to the ER. Another ER-PM MCS protein that we will focus on below is TMEM24 (C2CD2L). Anchored on the ER through its N-terminal transmembrane domain, it electrostatically interacts with the negatively charged phospholipids of PM through its polybasic C-terminal domain [117, 118]. It transports PI from the ER to the PM through a Ca<sup>2+</sup>-dependent mechanism. Elevations of Ca<sup>2+</sup> and DAG activate PKC which phosphorylates multiple targets, including the C terminus of TMEM24, resulting in neutralization of positive charges and the dissociation of TMEM24 from the PM. TMEM24 is highly expressed in pancreatic islets and its absence affects insulin secretion, indicating that lipid transfer is essential for normal insulin release [117, 118]. Pancreatic  $\beta$  cells lacking TMEM24 exhibit strongly suppressed glucose-induced Ca<sup>2+</sup> oscillations, indicating a connection between Ca<sup>2+</sup> and lipid signalling [117, 118].

## Membrane contact sites in $\beta$ cells

The ER is tightly associated with the mitochondria forming very dynamic crosstalk platforms termed mitochondria-associated membranes (MAMs). MAMs allow rapid exchange of biological molecules to maintain cellular

health. Although the contribution of MAMs in both normal  $\beta$ -cell function and in glucotoxicity-induced dysfunction remains largely unknown, recent studies have shown that the MAM integrity could be dynamically and differentially regulated in  $\beta$  cells during the progression of T2D pathology. Proximity-based assays revealed that palmitate-induced lipotoxicity in MIN6 cells decreases the number of IP3R1-VDAC1 interactions followed by increased expression of various markers of ER stress, as well as the decrease in insulin secretion in response to glucose [119]. Similarly, reduction of IP3R2-VDAC1 coupling was observed in  $\beta$  cells in pancreatic sections from patients with T2D [119]. MAMs in  $\beta$  cells need to be regulated in both time and space. Glucose stimulates mitochondrial  $\text{Ca}^{2+}$  uptake from the ER through MAMs [120], which can regulate mitochondrial ATP production [121]. Therefore, chronic disruption of the ER-mitochondria communication results in ER  $\text{Ca}^{2+}$  accumulation which leads to ER stress, alterations in the mitochondrial bioenergetics causing fission, and eventually to impaired glucose-stimulated insulin secretion [122]. High levels of  $\text{Ca}^{2+}$  in the mitochondria is also the cause of elevated expression of MICU1, and likely of MCU, in INS-1E cells. However, increased basal mitochondrial  $\text{Ca}^{2+}$  concentration makes the mitochondria prone to extensive fragmentation. Therefore, sustained organelle tethering is detrimental for the intracellular  $\text{Ca}^{2+}$  homeostasis and the overall  $\beta$ -cell function [123, 124].

## Membrane contact sites- associated diseases

Disruption of cellular inter-organelle communication networks connected by MCS can contribute to various diseases, such as cancer, neurodegenerative disorders and metabolic diseases [125-128]. It is important that alterations of MCSs are examined in the context of both the causal pathology but also incidental to other cellular dysfunctions as it is doubtful MCS account for all the aspects of a disease. The development of advanced microscopy and biochemical techniques enabled the discovery and exploration of the cell-type-specific molecular structure and the dynamic regulation of the MCSs. However, there is a high demand of better characterization of the MCSs in the healthy cells as they will allow better understanding of the MCS contribution to different disease pathologies. Disease-associated mutations might not affect the MCSs in a uniform fashion. ER-mitochondria contacts are increased in Alzheimer's disease (AD), but they are often decreased in Amyotrophic lateral sclerosis (ALS) and Parkinson's disease (PD) [129-132]. However, increase in the ER-mitochondria contacts have also been reported in both ALS and PD [133-137]. This highlights the importance of understanding the contextual regulation of MCS. Different underlying genotypes might be responsible for conflicting MCS alterations in the same disease as they might trigger direct abrogation of their function or compensatory increases in MCSs. In some cases, restoring MCS can rescue organelle function. For instance, Kim *et al.*, showed that in

Parkinson's disease patient-derived neurons, mitochondria-lysosome bidirectional crosstalk is an upstream regulator of mitochondrial function and dynamics, representing a promising therapeutic target [138]. Considering the fact that ER-PM, ER-mitochondria, and ER-Golgi contacts are regulatory sites for lipid metabolism and intracellular calcium homeostasis, some functions and interactions of MCS have been identified as mediators of the cancer cell metabolism during disease progression. Alterations of inter-organelle crosstalk in MAMs can lead to dysregulation of calcium signalling, which has been identified as a hallmark of cancer cells. In addition to that, dysregulated function of the MCSs components can lead to activation of oncoproteins such as AKT [139], PERK [140, 141], Grp75 [142], and VDAC [143, 144] and the inhibition of tumour suppressors such as p53 [145], the PTEN [146], and the PML [147, 148]. MCS changes have also been reported in response to chemotherapy treatments. However, the protection mechanism has solely been described in the context of restoration of calcium handling in the MAMs. It is believed that better characterization of the modulations of the processes carried out in MCSs that occur in cancer would favour the development of new and more efficient therapies for the inhibition of cancer progression.

## Membrane contact sites and type-2 diabetes

Type 2 diabetes mellitus (T2DM) is a complex endocrine and metabolic disorder, accounting for around 90% of all diabetes cases. It is characterized by insulin resistance in the peripheral tissue, skeletal muscle, liver or fat tissue, and involves impaired insulin secretion (IDF, 2020). As a consequence, there is 25–60% loss of pancreatic  $\beta$ -mass due to  $\beta$ -cell depletion and death [149, 150]. Aberrant loss of  $\beta$ -cell function and apoptosis are hallmarks of advanced T2D. Altered mitochondria structure [92], reduced mitochondrial respiration [151], decreased mitochondrial ATP production [152] and altered mitochondria dynamics [88] along with ER  $\text{Ca}^{2+}$  depletion [153] and activation of the unfolded protein response (UPR) [154] are several of the causal factors of  $\beta$ -cell failure. However, the exact causes of T2D and the precise molecular mechanisms involved is yet to be elucidated. Since MAMs are regulated by nutrient intake, it has been suggested that they are involved in the development of hepatic and muscle insulin resistance. ER-mitochondria contact number is decreased in the liver of fed compared to fasted mice [155]. In the human liver cell line HuH7, high glucose concentration or siRNA-mediated reduction of MAM components decrease the number of MAMs and induces mitochondrial fission [155]. These results highlight the role of MAMs in mitochondrial dynamics and nutrient-sensing in hepatocytes. In obese ob/ob mice or mice fed with a diet high in sugar and fat, the MAM numbers in liver cells are lower and accompanied by insulin resistance. *In vitro* and *in vivo* modulation of the expression of MAM-located proteins (Grp75, Mfn2 or CypD) further support a role of MAM in the development of hepatic insulin resistance [156, 157].

Consistently, improving MAM integrity in primary hepatocytes of diabetic mice restored hepatic insulin action. These studies highlight the importance of the adaptation of MAMs in different metabolic states for the correct response to insulin in hepatocytes. In addition to the liver, proper ER-mitochondria coupling is also essential for the insulin-sensing capacity of the skeletal muscle [156]. Experimental restoration of ER-mitochondria contacts in human myotubes prevents the effect of palmitate-induced alterations of insulin signalling and action. Differences in the MAM organization was also observed in human myotubes from obese subjects with or without T2D when compared to healthy lean subjects [156]. Overall, better understanding of the mechanisms behind the ER-mitochondria interactions is necessary as their disruption has been shown to precede the appearance of mitochondrial dysfunction and insulin resistance in the peripheral tissue. To date, no other type of organelle contacts has been reported for T2D.

## Phosphoinositides

In the eukaryotic cells, the organelles are physically and functionally separated by an elaborate membrane network which allows the compartmentalization of metabolic pathways and signalling cascades [158]. Phosphoinositides (PIs) are key determinants of membrane identity and serve as spatiotemporal cues to direct membrane dynamics [159-161]. PIs are a family of acidic phospholipids consisting of a glycerol backbone esterified to two fatty acid chains and a phosphate, and attached to a polar head group. The head group is a cyclic polyol myo-inositol which extends into the cytoplasm. PI synthesis starts in the ER and the delivery to other organelles occurs via either non-vesicular lipid exchange proteins in MCSs or through vesicular carriers in the secretory pathway [159]. Positions D3, D4 and D5 of the inositol head group can undergo reversible phosphorylation through the action of phosphoinositide kinases and phosphatases, generating seven combinatorically phosphorylated forms [159] (Figure 4). Although PIs are minor components of all eukaryotic cellular membranes, making up less than 1% of the total phospholipid pool of cells, there is tight spatiotemporal control of their synthesis and turnover [159]. For example, plasma membrane is enriched in PI(4,5)P<sub>2</sub> and, to a lesser extent, PI(4)P, while the Golgi network contains high levels of PI(4)P, and endo-lysosomal system is dominated by PI3P and PI(3,5)P<sub>2</sub>. Their highly specific subcellular distribution controls the organisation and activity of cytosolic and membrane-bound effector proteins (receptors, ion channels, transporters), and dynamic membrane remodelling and protein interactions enable rapid adaptations to environmental changes [162].





by the small GTPase ARF1 [163] and the giantin-interacting protein ACBD [164]. Although it is poorly understood how PI(4)P TGN levels facilitate the ER-to-Golgi transport, it has been shown that PI(4)P plays a central role in both clathrin-dependent and constitutive secretion. In the former case, PI(4)P contributes to the assembly of the clathrin adaptor proteins AP1, GGA1 and GGA2, which mediate transport from the TGN to endosomes and lysosomes [165, 166]. On the other hand, when associated with Golgi-localized phosphoprotein 3 (GOLPH3), myosin 18A, DOPEY1–MON2 complex, kinesin 1, 14-3-3 protein- $\gamma$ , the fission-promoting factors CTBP1/BARS27 and protein kinase D, PI(4)P promotes the formation of vesicular carrier of the constitutive secretory pathway [167-171], PI(4)P is also responsible for maintaining the distinct lipid composition of TGN which is enriched in glycosphingolipids, sphingomyelin and cholesterol. PI(4)P promotes the transfer of cholesterol and ceramide lipids to the TGN from the ER which, in turn, fuels the PI(4)P generation; ceramide along with phosphatidylcholine produce sphingomyelin leading to the formation of DAG [172]. Increased DAG levels activate PKD which induces the secretory carrier formation at the TGN and stimulate PI4KIII $\beta$  activity [173]. On the other hand, cholesterol supports palmitoylation and the TGN recruitment of PI4KII $\alpha$ , which in combination with PI4KIII $\beta$  promotes the PI(4)P synthesis from PIs [174]. PI(4)P is also shown to be a growth- and nutrient-sensing molecule. Upon serum starvation, secretion is suppressed via the PI(4)P-4-phosphatase (Sac1)-mediated reduction of the PI(4)P at the ER-TGN membrane contact sites [175]. The function of PI(4)P is further regulated by the cytoplasmic pH. Acidification of the intracellular environment causes protonation of phosphoesters in the lipid head group of PI(4)P, disrupting its interaction with PI(4)P binding effector proteins, which leads to suppressed secretory capacity [176]. In the plasma membrane, PI(4)P not only acts as the major source for the synthesis of PI(4,5)P<sub>2</sub>, but it contributes to the establishment of the negative charge in the inner plasma membrane leaflet of the plasma membrane promoting the electrostatic interactions with positively-charged amino acids of the membrane-associated proteins [177].

## The role of phosphoinositides in MCS formation

In some cases, the formation of MCSs is facilitated by PIs on the membrane of one organelle recruiting PI-binding proteins anchored to the opposite membrane. For example, MCS contacts can be partially stabilized via the recognition of PM-localized PI(4,5)P<sub>2</sub> by the lipid-binding C2 domains of the ER-localized Extended Synaptotagmins (E-Syts). E-Syts catalyse DAG transport from the PM to the ER where it may serve as a precursor for subsequent re-synthesis of PI. Other C2 domain-containing tethering proteins like TMEM24 can also contribute to the formation of ER-PM MCSs via the association with acidic lipids, e.g. PI(4,5)P<sub>2</sub>, in plasma membrane and transfer PIs under basal

conditions in  $\beta$  cells [117]. The OSBP-related proteins ORP5/8, which are lipid transfer proteins that interact with plasma membrane PI(4)P and PI(4,5)P<sub>2</sub> can also contribute to ER-PM MCS formation [178]. However, if bona fide tethering proteins at ER-PM contacts depend on interactions with PIs is still unknown. Additionally, PIs govern the formation of MCSs deeper in the cell. OSBP mediates lipid exchange at the ER-TGN interface where the PH-domain of OSBP associates with the PI(4)P on the TGN [179]. Lysosomal PI(3)P can be recognized by the FYVE domain-containing ER membrane protein protrudin and its associated factor PDZ domain-containing protein 8 [180]. PI(3)P also promotes the tethering of autophagic membranes to the ER via the interaction with the PROPPIN domain of WIPI4 [181].

## Cholesterol biosynthesis and function in $\beta$ cells

Cholesterol makes up 60-80% of plasma membrane lipids and plays a crucial role in determining the physical properties of the cell membranes, such as the fluidity and the curvature, which, in turn, affect the localization and function of plasma membrane proteins (i.e. transporters, ion channels and receptors) and support the formation of the secretory granules and their fusion with the lipid rafts in the plasma membrane [182]. Lipid rafts are microdomains of the plasma membrane consisting of cholesterol and sphingolipids, enriched in ion channels and receptors as well as proteins coupling glucose-sensing with insulin secretion [183]. Therefore, proper membrane structure is critical for the correct function of the pancreatic  $\beta$  cells. Cells can take up cholesterol via low-density lipoproteins (LDL) or through the reverse cholesterol flux pathway of high-density lipoproteins (HDL) [184, 185]. Cells can also synthesize cholesterol in the ER through the mevalonate pathway. Intracellular synthesis and extracellular cholesterol uptake are under the control of the transcription factor SREBP2 (sterol-responsive element binding protein 2) which regulates the transcription of the rate-limiting enzyme for cholesterol synthesis, hydroxymethylglutaryl-CoA reductase (HMGCoAR). SREBP2 is present in an inactive form, under basal conditions. Decrease of the cholesterol concentration or inhibition of its biosynthesis drive the activation of SREBP2, releasing it from the SREBP cleavage-activating protein (SCAP), a sterol-sensing molecule. SREBP2 translocates into the nucleus where it promotes the expression of HMGCoAR. In addition to that, it increases the expression of the low-density lipoprotein receptors (LDL-R) enhancing cholesterol uptake [186, 187]. SREBP2 overexpression leads to cholesterol accumulation, which results in reduced  $\beta$ -cell mass and impaired insulin secretion [187]. Excess cholesterol in  $\beta$  cells can be removed via the ATP-binding cassette transporter A1 (ABCA1)-mediated cholesterol efflux which transports cholesterol against its concentration gradient through ATP hydrolysis [187, 188]. In cells, cholesterol is heterogeneously distributed. The plasma membrane contains high

levels of cholesterol whereas the ER maintains low levels (5% mol) for several reasons [189, 190]. Besides the fact that cholesterol is transported to the other organelles from the ER via the OSBP activity, prolonged accumulation of cholesterol in the ER depletes the ER calcium stores and induces ER stress [191, 192]. The Golgi complex is enriched in cholesterol which favours the biogenesis and trafficking of secretory granules in pancreatic  $\beta$  cells [193]. Depletion of cholesterol destabilizes recently formed insulin granules, making them susceptible to degradation [194], while excess cholesterol accumulation leads to granule enlargement, alteration of insulin granule membrane protein composition, including clathrin accumulation, resulting in impaired exocytosis [193]. Plasma membrane-located lipid rafts, composed of cholesterol and sphingolipid-rich microdomains, act as spatial coordinators of the exocytic proteins included in the SNARE complex. Cholesterol depletion suppresses regulated exocytosis [195]. Therefore, cholesterol metabolism is tightly linked to  $\beta$ -cell function.

# Aims

- I. Determine the role of the lipid transfer protein TMEM24 in the regulation of  $\beta$ -cell function.
- II. Detect putative ER-insulin granule membrane contact sites and determine the role of oxysterol-binding protein OSBP-mediated cholesterol transport at these sites.
- III. Identify distinct stages of early insulin granule maturation in  $\beta$  cells

# Methodology

## Pancreatic $\beta$ -cell models

During the past 40 years, several studies have aimed at understanding how  $\beta$  cells develop, function, grow, and die, using rodent models either *in vivo* or *in vitro*. To date, in addition to rodent islets, immortalized  $\beta$ -cell lines, such as the rat insulinoma cells (RIN), hamster pancreatic b-cells (HIT), transgenic C57BL/6 mouse insulinoma cells (MIN),  $\beta$ -tumour cells (bTC), and rat insulinoma cells (INS-1) have been used to investigate pancreatic  $\beta$ -cell physiology [196]. The establishment of these insulin-secreting cell lines benefited vastly the  $\beta$ -cell research field as it allowed the investigation of how the  $\beta$  cells produce, store and secrete insulin by providing essentially unrestricted access to functional  $\beta$  cells.

The different *in vitro*  $\beta$ -cell models that we used in our studies involve MIN6 clonal  $\beta$  cells, MIN6 pseudoislets, and mouse islets of Langerhans. The MIN6 cell line is derived from targeted oncogenesis in transgenic mice expressing the large-T antigen of simian virus (SV40T antigen) under the control of the insulin promoter [197]. The formation of tumours resulted in the generation of the MIN6 cell line. The main advantages of MIN6 cells are the maintenance of a differentiated phenotype for several passages in culture and the high degree of insulin secretions upon glucose stimulation [197]. They also share many upstream signal transductions and second messenger signalling pathways with primary  $\beta$  cells. MIN6 cell cultures can be easily maintained, transfected and infected which was very beneficial to our fluorescence-based observations at single cell level. In addition to the two-dimensional cell culture, we included in our studies observations from MIN6 pseudoislets, which are three-dimensional islet-like cell clusters that develop when cell-to-cell contact is re-established after MIN6 cells reaggregate in suspension. MIN6 pseudoislets not only mimic the architecture of primary islets [198-202] but, maybe, most importantly, demonstrate enhanced secretory capacity compared to MIN6 monolayer cultures [203]. This might be the outcome of improved intra- and intercellular communication of the cells inside the islet-like structures, for example enhanced synchronized insulin secretion mediated by the presence of gap junctions [204].

Although the cell lines have the advantages of unlimited growth and relative ease of transfection or genetic modification, isolated islets and individual

primary  $\beta$  cells are considered to be the most relevant model to investigate  $\beta$ -cell function. For our studies, the mouse pancreas was dissected out and subjected to collagenase digestion to isolate islets of Langerhans [205].

## Live cell imaging

Fluorescence microscopy (FM) has enabled the visualization of cellular processes, and, therefore, increase our understanding of cell physiology and pathophysiology; key elements in cell biology research. FM-based investigation requires the use of fluorescent protein (FP) tags or dyes (fluorophores) to label the protein or subcellular compartments of interest. Based on the spatiotemporal resolution requirements, scientists can choose among wide-field, multiphoton, laser scanning confocal, spinning disk confocal or total internal reflection fluorescence (TIRF) microscopy [206] (Figure 5). The last two categories allow monitoring living cells for extended time periods thanks to low phototoxicity and reduced photobleaching, processes that can otherwise negatively affect the status of the cells and the fluorophores [207]. In our experiments, we used the most common fluorescent tags including GFP, mNeon-Green and the red fluorescent protein (RFP). In addition to those, we fused self-labelling protein tag (HaloTag) with some of our proteins of interest.

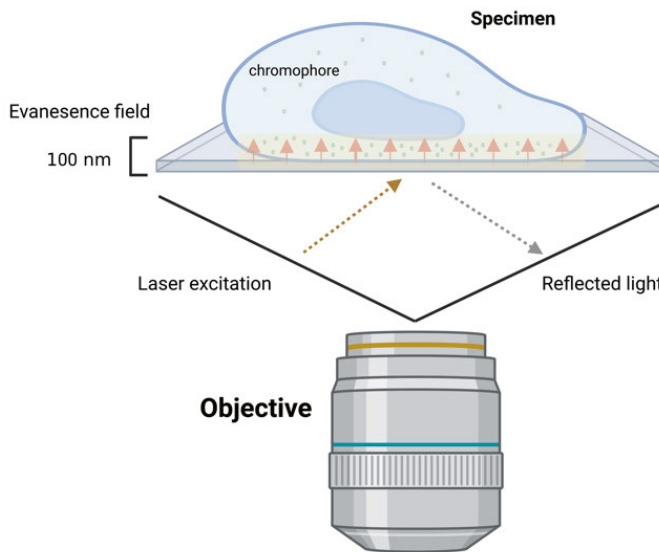


Figure 5: Schematic overview of the TIRF microscopy principle.

Confocal and TIRF microscopy are the two main methods in our studies. Regarding the first, the lateral resolution of ~200 nm and axial resolution of 500 nm allows for monitoring a plethora of subcellular events and the distribution of our target molecules. The presence of the pinhole (or multiple pinholes in the case of spinning disk microscope) in the emission light pathway eliminates the unfocused light to be detected by the camera. Here, I used both types of confocal microscopy: laser-scanning confocal microscopy (LSCM) and spinning disk confocal microscopy (SDCM). Using a focused beam to scan the specimen, LSCM generated high-resolution images. This method is best suited for fixed samples due to the high light dose, but less appropriate for live cell imaging. This obstacle is overcome by the SDCM, where multiple pinholes present on a Nipkow disk are used to scan the specimen. These allow rapid acquisition in combination with low phototoxicity and photobleaching. TIRF microscopy is ideally suited for monitoring events close to the plasma membrane as the evanescent field is restricted to 100 nm from the coverslip - plasma membrane interface [208]. These properties make this technique especially well-suited for studies on e.g. endocytosis and exocytosis, which are critical for the normal function of  $\beta$  cells.

## Ca<sup>2+</sup> imaging techniques and indicators

The understanding of the underlying mechanisms of Ca<sup>2+</sup> signalling has been facilitated by the development of fluorescent Ca<sup>2+</sup> indicators [209]. In  $\beta$  cells, intracellular Ca<sup>2+</sup> has a central role in the regulation of insulin secretion. The study of Ca<sup>2+</sup>-mediated processes has been greatly facilitated by the broadly available Ca<sup>2+</sup> indicators with optimized binding affinity properties and subcellular localization. Generally, there are two classes of Ca<sup>2+</sup> indicators; genetically encoded fluorescent proteins and chemically engineered fluorophores.

One major criterion when selecting a Ca<sup>2+</sup> indicator is usually the spectral properties of the fluorophore. Based on this feature, the chemical Ca<sup>2+</sup> indicators can be categorized as either ratiometric or single wavelength indicators. In the first ones, there is a shift in the peak of either the excitation or emission wavelength upon Ca<sup>2+</sup> binding, providing more accurate Ca<sup>2+</sup> measurements, corrected for dye loading, leakage and photobleaching. The latter category includes Ca<sup>2+</sup> indicators that demonstrate Ca<sup>2+</sup>-dependent changes at a single wavelength, which minimizes the chances for spectral overlap with other fluorophores that might be included in the experimental set up [210-213]. Their main advantage over the genetically encoded ones is the broad spectrum of Ca<sup>2+</sup> affinity and the ease by which they can be introduced into cells following well-established protocols [214]. The lipophilic nature of these dyes was the outcome of their engineering with acetoxymethyl (AM) esters.

However, their subcellular distribution cannot be controlled and their restriction to a specific organelle is nearly impossible. In addition to that, over time, the chemical  $\text{Ca}^{2+}$  indicators tend to compartmentalize and be extruded from the cells [215, 216]. The dissociation constant ( $K_d$ ) reflects how strongly the dye binds  $\text{Ca}^{2+}$  [217]. Cytosolic  $\text{Ca}^{2+}$  concentration in the  $\beta$  cell ranges from 100 nM, under resting conditions, up to a few micromolar upon stimulation [218]. Therefore, some of the suitable cytosolic  $\text{Ca}^{2+}$  indicators for studies on  $\beta$ -cell function include Fluo-4 ( $K_d$  335 nM), Fura-2 ( $K_d$  161 nM) [219] and cal520 ( $K_d$  320 nM) [217].

The genetically encoded  $\text{Ca}^{2+}$  indicators are categorized into the Förster resonance energy transfer (FRET)-based chameleon type [220] and the single GFP type [221]. Currently, the most popular indicator (GCaMP) belongs to the second category. It is a single-fluorophore sensor consisting of the green fluorescent protein (GFP), or other fluorescent variants, fused to the calmodulin (CaM) binding region and the M13 domain of myosin light chain kinase. Upon  $\text{Ca}^{2+}$  binding, CaM and M13 interact leading to an increase of GFP fluorescence. Moreover, new indicators with improved  $\text{Ca}^{2+}$  binding and fluorescence properties have been recently developed [221]. Among them, R-GECOs have red-shifted absorption and emission spectra [222]. In contrast to chemical dyes, they need to be delivered into the intracellular compartments through transfection or viral transduction, followed by a short incubation period before imaging. The main advantage, however, is that they can be targeted to specific organelles (using organelle targeting sequences) or cell-types (using cell-type specific promoters). In our studies below, we used two genetically encoded  $\text{Ca}^{2+}$  indicators. For the mitochondrial  $\text{Ca}^{2+}$  measurements, we used LAR-GECO1.2 ( $K_d$  12  $\mu\text{M}$ ) which is a low-affinity red fluorescent indicator fused with the cytochrome C oxidase VIII sequence to target the expression of the sensor into the mitochondrial matrix. For the ER  $\text{Ca}^{2+}$  measurements, we used a FRET-based genetically encoded calcium indicator, D4ER, which contains an engineered low-affinity CaM-M13  $\text{Ca}^{2+}$  binding region that links two fluorescent proteins (CFP/YFP). Upon  $\text{Ca}^{2+}$  binding, the association of CaM-M13 increases the energy transfer between CFP and YFP [223].

## Insulin secretion measurement *in vitro*

There are several methods to measure insulin secretion from  $\beta$ -cell monolayers, aggregates (pseudo-islets) or isolated pancreatic islets of Langerhans. In the studies included in this thesis, we used an antibody-based detection assay called enzyme-linked immunosorbent assay (ELISA) to measure insulin release from either the supernatant of  $\beta$ -cell monolayer or islets. The insulin concentrations were normalized against the total insulin content.

There are also several techniques to monitor the secretion profile of insulin at the single-cell level. Using cells expressing the pH-sensitive Vamp2-



pHluorin coupled with TIRF microscopy, it is possible to follow the dynamics of fusion events of insulin vesicles with the plasma membrane of  $\beta$  cells. More specifically, the pHluorin is a genetically encoded optical reporter suitable for monitoring pH changes. Developed by Miesenböck and coworkers, following a histidine combinatorial mutagenesis strategy and pH-related screening, they developed new variants of GFP (pH-sensitive green fluorescent protein-based sensors) which enabled measurements of dynamic changes in pH of vesicle lumen resulting from exocytosis and endocytosis events. More specifically, the acidic lumen of the vesicles (pH 5.0) maintains the reporter at a quenched state. Upon stimulation, the insulin granules fuse with the plasma membrane to release insulin. During fusion, the luminal surface of the vesicle is exposed to the more alkaline pH of the extracellular environment (pH  $\sim$ 7.4) making the externalized pHluorin brightly fluorescent. Under TIRF microscopic examinations, the fusion events are observed as “flashes” and can be easily quantified. However, this method does not distinguish between exocytosis and endocytosis events and it only reflects changes in the secretion but does not allow the quantification of absolute amounts of insulin released.

## Visualization of membrane contact sites

The first observation that organelles do not operate as single units but are parts of a fine-tuned network came in the 1950s. EM revealed the juxtapositions of mitochondrial and ER membranes in rat liver cells [224]. However, it took another 35 years before they were shown to play a significant role in lipid transport from the ER to mitochondria, at which point the contacts received the name “MAMs” (mitochondria-associated ER membranes). Nowadays it is well established that MAMs provide a platform that is fundamental for several cellular functions, such as calcium homeostasis, autophagy, apoptosis and lipid metabolism [225-227].

Today, there is a versatile toolbox for studying membrane proximity. The first category of experimental approaches consists of biochemical and electron microscopy (EM)-related methods. These are commonly used for the morphological characterization of the contacts and the identification of the molecular players. The second includes a wide variety of proximity-driven fluorescent probes which provide spatiotemporal details and support studies on the function and dynamics of MCSs in fixed cells but also in living cells under specific cellular conditions or upon stimulation.

In the study of MCSs, microscopy-related techniques allow studying the architecture of inter-organelle membrane tethering. Using transmission electron microscopy (TEM), a beam of electrons is transmitted through an ultrathin section of the specimen and forms a high-resolution image of subcellular compartments of interest [228]. In scanning EM (SEM), the beam of high-energy electrons can generate a variety of signals related to the surface

of the irradiated sample, enabling reconstruction of detailed 3D structures of cellular subdomain [229]. Focused ion beam-SEM (FIB-SEM) is a technology developed around SEM where a second gallium ion beam is added to ablate the material between two acquisitions performed by SEM [229]. This approach provides 3D images of regions of interest in the cell at a nanometer scale. However, due to potential complications during sample preparation, the fact that these methods are time- and cost-intensive as well as the limitation of studies to fixed cells, fluorescent microscopy-based assays are more frequently used for studying MCS.

In MCS studies, proximity-driven fluorescent probes can overcome the spatial resolution limit of conventional microscopy (lateral resolution  $\sim 200$  nm and axial resolution  $\sim 500$  nm), as the fluorescence signal is generated and amplified locally upon the membrane proximity of the organelles. This category includes PLA-, FRET-, BiFC-, and ddFP-based probes. Proximity ligation assay (PLA) is mainly employed to visualize interacting proteins within 40 nm *in situ* [230] and was recently applied to identify membrane contacts [231]. The proximity of two antibodies recognizing target epitopes on opposite membranes allows the subsequent hybridization of oligonucleotide-conjugated secondary antibodies (PLA probes). The connectors serve as primers for the generation of the Rolling Circle Amplification (RCA) product that can be visualized after the addition of labelled oligonucleotides that bind the amplified DNA molecules [230]. The generation of PLA dots allows the identification of specific proteins interacting at the interface between e.g. two organelles at a maximal distance of 40 nm. The established protocol requires fixation of the cells which precludes studies in living cells.

FRET-, BiFC-, ddFP-based sensors allow the observation of membrane contact sites *in situ* and in living cells. Based on the Fluorescence resonance energy transfer (FRET) principle, where a donor fluorophore when excited can transfer its energy not only intramolecularly but also intermolecularly to an acceptor molecule at a distance of up to 10 nm [232], the probes of the first category can monitor protein-protein interactions with a high spatial resolution when fused to the proteins that function in the MCSs. The Bimolecular fluorescence complementation (BiFC) approach is based on the reconstitution of a fluorescent complex by two non-fluorescent fragments. Moreover, the addition of spacers with various lengths can provide more accurate information regarding the distance of the interacting proteins. This complex formation is generally irreversible and its stability allows the real-time detection of low-affinity interactions at narrow distances, but precludes visualization of contact site dynamics. In our studies, we employed the dimerization-dependent fluorescent protein (ddFP). The ddFPs derive from homodimeric *Drosophila* red fluorescent protein (DdRed). The fluorescent signal significantly increases upon dimerization of the two non-fluorescent moieties. Alford and colleagues expanded the palette, by engineering the progenitor red (ddRFP) variant, to include green (ddGFP) and yellow (ddYFP) variants [233]. These

highly effective indicators not only presented an increased *in vitro* contrast and brightness but most importantly they had a modest reciprocal affinity making the system suitable to investigate rapid inter-organelle crosstalk [234].

## Visualization of cholesterol

Cholesterol is a major structural component of cell membranes. Cholesterol synthesis and distribution in the different organelle membranes is tightly regulated as it can drastically affect the membrane properties [235]. In the ER membrane, cholesterol levels cannot exceed 0.5-1% as they can affect negatively the protein folding [235]. On the contrary, cholesterol is enriched in the plasma membrane as a consequence of efficient transport from the ER [236]. Fluorophore-labelled cholesterol, such as BODIPY (Bora-diaza-indacene)-cholesterol and TopFlour-Cholesterol (dipyrrromethene difluoride (BODIPY)-labelled sterol analogue) are the most widely employed fluorescent molecules used to monitor sterol uptake and inter-organellar membrane distribution in living cells. However, the addition of exogenous fluorescent sterol analogue might result in aberrant localization or function [237]. Moreover, in fixed cells, filipin, a polyene antibiotic, can be used to visualize free (un-esterified) cholesterol as it binds  $3\beta$ -hydroxysterols of the membranes. This perturbation of the bilayer makes the method suitable only for fixed samples. An additional challenge stems from the fluorescence properties of Filipin. Having an excitation peak at the 360 nm and emission at 480 nm, there is rapid photobleaching in specimens making the acquisition of high-resolution images challenging [238].

# Results and discussion

## Paper I

Membrane contact sites have been extensively investigated as they play a crucial role in intracellular lipid trafficking and calcium signaling. They can be maintained by tethering proteins and can serve as sites for non-vesicular lipid exchange between two organelles, mediated by lipid transport proteins (LTPs). In  $\beta$  cells, ER-PM junctions are essential since they are used to replenish PM phosphatidylinositol (PI), which is the precursor molecule for phosphatidylinositol-4-phosphate (PI(4)P) and phosphatidylinositol 4,5-bisphosphate (PI(4,5)P<sub>2</sub>), two lipids of importance for normal insulin secretion [239, 240]. Glucose stimulation can trigger both calcium- and lipid- dependent signaling cascades that result in the release of insulin into the bloodstream. Glucose uptake and metabolism increases the ATP/ADP ratio which results in closure of the ATP-sensitive K channels, PM depolarization and the consecutive opening of voltage-dependent Ca<sup>2+</sup> channels. Ca<sup>2+</sup> subsequently triggers insulin granule fusion with the PM [241]. Although cytosolic Ca<sup>2+</sup> is, without doubt, the most important regulator of insulin granule exocytosis, phosphoinositides can affect multiple aspects of the insulin secretion mechanism, including membrane depolarization, Ca<sup>2+</sup> influx and granule docking and release [242]. In addition to this, PI(4,5)P<sub>2</sub> can be hydrolyzed by PLC into inositol 1,4,5-trisphosphate (IP<sub>3</sub>) and diacylglycerol (DAG) which triggers Ca<sup>2+</sup> release from the ER and PKC activation, respectively [243, 244].

TMEM24 (C2CD2L) is a recently identified LTP that provides the PM with PI. Anchored at the ER membrane through its N-terminal transmembrane domain, it dynamically localizes at the ER-PM MCSs where it stabilizes through electrostatic interactions between its C-terminal polybasic region and negatively charged lipids in the PM. This tethering behavior is dynamic and regulated by Ca<sup>2+</sup>-dependent phosphorylation by PKC which neutralizes the positively charged surface of TMEM24, resulting in its dissociation from the PM [117]. When bound to the PM, TMEM24 facilitates PI transport through an N-terminal synaptotagmin-like mitochondrial-lipid-binding (SMP) domain from the major site of synthesis, ER, to the PM, and provide the precursor for PI(4,5)P<sub>2</sub> and PI(4)P synthesis. TMEM24 is highly expressed in neurons and pancreatic islet cells [117, 118]. Previously, in INS-1 cells, TMEM24 was shown to be essential for the generation of glucose-induced Ca<sup>2+</sup> oscillations and insulin secretion [117, 245]. However, since TMEM24 is spatially

separated from the insulin secretion process during glucose elevation, it is unclear how it contributes to secretion regulation.

### Distribution of TMEM24 is controlled by DAG and $\text{Ca}^{2+}$

To investigate the mechanism by which TMEM24 regulate insulin secretion in  $\beta$  cells, it was first important to determine the conditions that induce TMEM24 dissociation from the PM. Transient expression of GFP-tagged TMEM24 in MIN6 cells loaded with the  $\text{Ca}^{2+}$  indicator Cal590 allowed monitoring of TMEM24 subcellular redistribution along with the changes in the cytosolic  $\text{Ca}^{2+}$  concentration. Using TIRF microscopy, we observed that elevation of the glucose concentration from 3 mM to 20 mM or direct membrane depolarization with 30 mM KCl caused a reduction of TMEM24-GFP fluorescence at the PM, indicating TMEM24 dissociation. Similarly, both  $\text{IP}_3$ -mediated release of  $\text{Ca}^{2+}$  from the ER and the passive ER  $\text{Ca}^{2+}$  depletion resulted in loss of TMEM24 from the PM, indicating that this process is  $\text{Ca}^{2+}$  regulated. Intriguingly, TMEM24 has been recently identified as a PKC target which can be activated not only by  $\text{Ca}^{2+}$  but also DAG. Under resting conditions, DAG levels in the PM are low and, upon glucose stimulation, DAG is removed from the PM through E-Syt-mediated transport at ER-PM contacts [246]. Addition of the DAG analogue phorbol 12-myristate 13-acetate (PMA), similar to  $\text{Ca}^{2+}$  increases, also induced TMEM24 dissociation from the, showing that  $\text{Ca}^{2+}$  and DAG can independently trigger TMEM24 removal from ER-PM MCSs. Results from permeabilized cells indicated that TMEM24 was partially dissociated from the PM under resting conditions due to constitutive PKC activity, and further dissociation occurred upon elevation of cytosolic  $\text{Ca}^{2+}$  in the high nanomolar to micromolar range. These observations are consistent with parallel actions of TMEM24 in a separate spatial context, possibly away from the ER-PM junctions (Figure 6).

### TMEM24 supports sustained insulin secretion and regulate ER $\text{Ca}^{2+}$

MIN6 cells cultured in monolayer, with either siRNA-mediated knockdown (KD) or CRISPR/Cas9-mediated knockout (KO) of TMEM24, exhibited normal glucose- and depolarisation-induced  $\text{Ca}^{2+}$  oscillations and insulin secretion. Control cells stimulated with 20 mM glucose showed a transient lowering of the cytosolic  $\text{Ca}^{2+}$  concentration due to ATP-driven sequestration of the ion into the ER [247]. This response was lacking in TMEM24 KD and KO cells, indicating an inability of the ER to take up  $\text{Ca}^{2+}$ . However, in all cell types, prolonged stimulation with 20 mM glucose caused  $\text{Ca}^{2+}$  increases and sustained generation of  $\text{Ca}^{2+}$  oscillations. Furthermore, we performed  $\text{Ca}^{2+}$  and insulin secretion measurements in pseudo-islets, which are spherical  $\beta$ -cell

clusters where electrical coupling between cells is enabled. As a result, they can imitate better the conditions of primary  $\beta$ -cells in pancreatic islets. The pseudo-islets that were constituted from wild-type MIN6 cells demonstrated a normal biphasic insulin secretion pattern as a response to a step increase in glucose from 3 mM to 20 mM glucose. This time course was composed of an initial peak of insulin secretion followed by a sustained phase with slower release rate. Interestingly, there was significant impairment of the sustained insulin secretion during the second phase in the TMEM24 KO pseudo-islets, supporting a regulatory role of TMEM24 during sustained insulin secretion, which is at odds with previous reports showing an absolute requirement of TMEM24 for both phases of insulin secretion [117, 245]. This can be explained by the use of different experimental set ups and  $\beta$ -cell models.

The absence of initial lowering in the cytosolic  $\text{Ca}^{2+}$  concentration upon glucose stimulation in cells with reduced TMEM24 expression was an indication that this protein may affect the ability of the ER to sequester or store  $\text{Ca}^{2+}$ . To further evaluate the effect of TMEM24 in ER  $\text{Ca}^{2+}$  homeostasis, the cytosolic  $\text{Ca}^{2+}$  levels were measured following ER  $\text{Ca}^{2+}$ -store depletion using the SERCA pump inhibitor CPA in a  $\text{Ca}^{2+}$ -free buffer. We found that TMEM24 KO cells have increased  $\text{Ca}^{2+}$  accumulation in the ER. Generally, an explanation for the ER  $\text{Ca}^{2+}$  sequestration in the TMEM24 KO cells could be an enhanced activity of the SERCA pump or reduced ER  $\text{Ca}^{2+}$  leak. However, it cannot explain the observations that the initial lowering of  $\text{Ca}^{2+}$  upon glucose stimulation was absent in TMEM24 KO cells. Since ER  $\text{Ca}^{2+}$  sequestration is an energy-demanding process, ATP production could be impaired in the TMEM24 KO cells.

## TMEM24 regulates mitochondrial $\text{Ca}^{2+}$ homeostasis and ATP production

Upon glucose uptake, glycolysis and mitochondrial metabolism, the generated ATP is used to fuel  $\text{Ca}^{2+}$  extrusion and organellar sequestration, in order to maintain the resting cytosolic  $\text{Ca}^{2+}$  concentration close to 100 nM. These mechanisms are particularly important in  $\beta$  cells, where regular elevations of the cytosolic  $\text{Ca}^{2+}$  are triggers for insulin granule exocytosis. In addition to  $\text{Ca}^{2+}$  measurements, mitochondrial function was assessed directly with the Seahorse XF technique and the fluorescent mitochondrial membrane potential indicator TMRM. Even though wild-type cells and TMEM24 KO cells showed no difference in their mitochondrial morphology, the oxidative phosphorylation in the latter was impaired under high glucose levels. In addition to that, the inner mitochondrial membrane was partially depolarized. Direct  $\text{Ca}^{2+}$  measurements in the organelle, using the mitochondrially targeted  $\text{Ca}^{2+}$  indicator LAR-GECO1.2, showed hyper-accumulation of  $\text{Ca}^{2+}$  in the organelle in TMEM24 KO cells following cytosolic  $\text{Ca}^{2+}$  concentration increases.

Therefore, combining all our observations, we explored the possibility that TMEM24 functions at MCSs distal to ER-PM junctions. Following depolarization-induced  $\text{Ca}^{2+}$  influx, TMEM24 dissociated from the PM and was instead found to be enriched on the mitochondria. To test if TMEM24 specifically localized to ER-mitochondria MCS, we co-expressed a dimerization-dependent fluorescent protein that reports contact sites between ER and mitochondria. Consistent with a role of TMEM24 at ER-mitochondria MCS, we found overlap between the reporter and TMEM24 that was enhanced following depolarization. However, the potential TMEM24-mediated transport of PI to the outer mitochondrial membrane needs to be further explored. Interestingly, Rosivatz and Woscholski showed that lower levels of  $\text{PI}(4,5)\text{P}_2$  on the outer mitochondrial membrane caused fragmentation of the organelle [248]. This was prevented by PKC activation which among other things induces the TMEM24 dissociation from the PM. This highlights the significance of controlling the mitochondrial function, especially in the energy-dependent environment of the  $\beta$  cells where ATP production influences the cytosolic and organellar  $\text{Ca}^{2+}$  homeostasis and, therefore, the efficiency of insulin secretion.

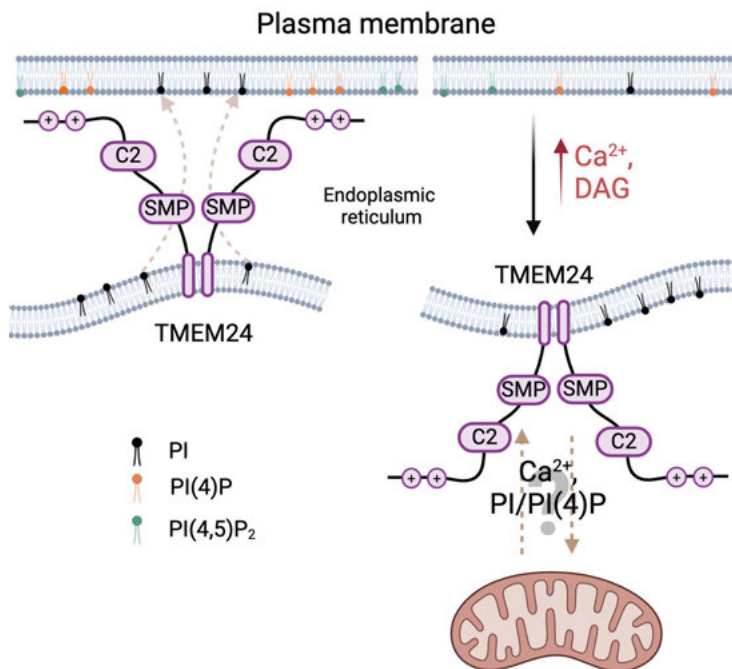


Figure 6: TMEM24 interacts with the plasma membrane and dissociates in response to both diacylglycerol and nanomolar elevations of cytosolic  $\text{Ca}^{2+}$ , becoming accessible at sites proximal to mitochondria. TMEM24 may influence mitochondrial function directly either by controlling the transfer of  $\text{Ca}^{2+}$ /PI/PI(4)P.

## Paper II

Insulin secretion is a multi-step process comprised of insulin biogenesis, granule transport and exocytosis. The protein and lipid composition of the granule at a prevailing stage ensures proper cargo loading and granule maturation, and PIs constitute one important class of granular lipids. However, the relative proportion of different PI species on the surface of insulin secretory granules (ISGs) as well as their functions are not known [249]. Due to their *trans*-Golgi network (TGN) origin, granules have high concentration of PI(4)P in their membranes which is required for the formation of transport vesicles [250, 251]. In yeast, vesicular PI(4)P has been previously shown to promote myosin-dependent granule transport [252] and by being removed it ensures efficient fusion with the plasma membrane. The levels of PI(4)P on organellar membranes can be controlled by the action of PI4-kinases and PI(4)P-phosphatases. In our lab, we recently revealed the presence of the PI(4)P-phosphatase Sac2 on the surface of ISGs and highlighted its contribution to granule maturation and exocytosis [253]. Lack of Sac2 caused impaired fusion of insulin granules with the PM and, thus, a reduction of insulin secretion [253]. In contrast to TGN and ISGs, the levels of PI(4)P in ER are very low as a result of the constitutive activity of the PI(4)P-phosphatase Sac1. The PI(4)P gradients between the ER and other organelle membranes serve as the energy source for vectorial transfer of other lipids during non-vesicular lipid transport. At the TGN-ER contact sites, the transport of one cholesterol molecule from the ER to the TGN, via the oxysterol-binding protein (OSBP), costs one PI(4)P which is counter-transported and hydrolysed by ER-localized Sac1. Because of PI(4)P hydrolysis after the back transfer, the process is irreversible and establishes a cholesterol gradient between the apposed membranes [112, 254]. To what extent OSBP could function as a rapid PI(4)P/cholesterol exchanger at the interface between ER and ISGs is not known. However, previous studies showed that loss of the mammalian Osh4p homologue OSBP had a negative impact on the insulin secretion [194]. Together with the crucial role of cholesterol accumulation on the ISGs for the efficiency of insulin release indicated the presence of an OSBP-mediated cholesterol transfer from the ER to the ISGs.

### Detection of contact sites between the ER and the ISGs

In the study of MCSs, the first critical point is the choice of the visualization technique. Since MCSs between the ER and ISGs have never been described before, EM-based approaches were used for the detection of possible ER-ISG-membrane proximity. Traditional transmission electron microscopy revealed ER-ISG contacts in mouse and human  $\beta$  cells. The volumetric reconstruction of individual ER-granule contacts using Focused Ion Beam Scanning Electron



Microscopy (FIB-SEM) of mouse  $\beta$  cells allowed us to visualize with high-resolution ribosome-free ER domains in close apposition to ISGs.

Even though EM-based techniques are powerful for visualizing the morphology of these subcellular compartments, proximity-driven fluorescent probes can provide additional information on the identity of the interacting components at these sites, and at the same time overcoming the spatial resolution limit of conventional microscopy. The proximity ligation assay (PLA) was used to visualize interactions between ER-localized proteins (VAP-A or Sec61b) and the ISG-localized effector protein (Rab3). Upon proximity of the protein complex of interest, the oligonucleotide-conjugated secondary antibodies hybridize. This promotes the production of an amplicon through the Rolling Circle Amplification (RCA) reaction that can be detected through the binding of a fluorescent probe at multiple positions of the RCA product. The generation of PLA dots allowed the identification of specific components involved in the assembly of ER-ISG tethers, interacting at a maximal distance of 40 nm. The number of PLA dots was markedly higher in the mouse primary  $\beta$ -cells compared to the MIN6 clonal  $\beta$  cells, possibly reflecting higher ISG density in these cells.

By definition, membrane contact sites (MCSs) correspond to a distance 10-35 nm between the membranes of the apposed organelles [106]. PLA did not secure the distance limit between the interacting molecules and also did not permit the study of the putative dynamics of ER-ISG CSs in living cells. To overcome these obstacles, a dimerization-dependent fluorescent reporter was developed. It consists of two non-fluorescent monomers, RA and GB, that form a fluorescent dimer upon proximity [233]. By targeting molecules that participate in the well-characterized ER-PM contacts, the maximal distance for the reconstitution of the fluorescent protein was determined to be smaller than 20 nm which is consistent with typical inter-membrane distance at MCSs [106]. Expression of ER-localized RA (RA-Sec61 $\beta$ ) and granule-localized GB (GB-Rab3) resulted in the detection of punctate fluorescent signal that colocalized with markers of both the ER (ER-oxGFP) and a subset of ISGs (NPY-mNG). Live-cell imaging revealed the dynamic behavior of these MCSs, supporting a physical tethering of the two organelles and not just stochastic proximity.

## OSBP localizes to ER-ISG contact sites in a PI(4)P-dependent manner

Since VAP-A was indicated to participate in the ER-ISG contacts based on the PLA results described above, we hypothesized that there is a PI(4)P/cholesterol transport catalysed by the lipid transport protein (LTP) oxysterol-binding protein (OSBP) [19, 20]. OSBP was previously described to bind to PI(4)P in the TGN membrane via the N-terminal pleckstrin homology (PH) domain and to the ER through an interaction between VAP-A and its FFAT

(two phenylalanines in an acidic track) motif [19, 20]. Transient expression of OSBP in MIN6 cells demonstrated its distribution mainly to the TGN and to a lesser extent on the plasma membrane and in the cytosol. Interestingly, incubation of the cells with the OSBP inhibitor OSW-1 had an immediate effect on the subcellular distribution of OSBP. More specifically, OSBP was stabilized at PI(4)P-rich membranes, including punctate structures in the cytosol. A similar pattern was seen for endogenous OSBP in both mouse and human pancreatic islet cells, and co-immunostaining against insulin revealed that the cytosolic structures were ISG. This observation agreed with live-cell imaging data, where ISG markers (NPY-mCherry or NPY-mNG) and fluorescently tagged OSBP (OSBP-GFP or OSBP-Halo<sup>JF646</sup>) were co-expressed in MIN6 cells. Under resting conditions, OSBP localized to the TGN. Upon OSW-1 treatment, OSBP became enriched on the ISGs. Expression of the PH domain from OSBP together with the ISG marker showed a similar pattern, indicating that the interaction between OSBP and ISGs was PI(4)P-dependent. OSW-1 treatment had no impact on the VAP-A distribution and the overall morphology of the ER network. The effect of OSW-1 on the OSBP distribution was strikingly prevented by the broad PI4-kinase inhibitor phenylarseneoxide (PAO) but not by the more selective class III $\beta$  (PIK93 and PI4KI) or class III $\alpha$  (GSK-A1) inhibitors, making class II $\alpha$  PI4-kinases a possible candidate for PI(4)P synthesis in the ISGs membrane. Consistent with this, results from immunostainings and live cell imaging showed the presence of class II $\alpha$  PI4-kinases on ISGs.

To examine further the subpopulation of ISGs that OSBP interacted with, we co-expressed OSBP-Halo<sup>JF646</sup> with the ER-ISG proximity reporter and VAPA-mNG. Consistent with the previous observations, OSBP localized to TGN under resting conditions and stabilized at ER-ISG contact sites upon OSW-1 treatment. By fusing OSBP to the GB monomer and co-expressing the construct together with the RA-Sec61 $\beta$  and a ISG marker (NPY-mNG) in MIN6  $\beta$ -cells, we observed the appearance of detectable puncta that overlapped with the ISGs after inhibiting the OSBP-mediated lipid exchange. This observation supports further the enrichment of OSBP between the membranes of ER and IGs in OSW-1 treated cells.

## OSBP binding to ISGs is regulated by Ca<sup>2+</sup> and cytosolic pH

The transient enrichment of OSBP on the ISGs upon OSW-1 addition motivated additional investigations of conditions that would provoke similar effect. Ca<sup>2+</sup> influx upon glucose stimulation is the major trigger of insulin secretion. As a result, it plays a crucial role in the function of  $\beta$ -cells. Elevated cytosolic Ca<sup>2+</sup> concentration prevented OSBP binding to the TGN, possibly as a result of lower PI(4)P kinases activity and, thus, reduced PI(4)P levels on the Golgi membranes [255, 256]. Experiments using both confocal and TIRF microscopy revealed that depolarization-induced increase of cytosolic Ca<sup>2+</sup>

caused rapid dissociation of the OSBP from the TGN. This was reversed upon wash-out of the depolarizing agent. Similarly, carbachol, via IP<sub>3</sub>-mediated release of ER Ca<sup>2+</sup>, caused the removal of OSBP from the TGN. Therefore, it is possible that increases in cytosolic Ca<sup>2+</sup> released OSBP from the ER-TGN contacts, making it available for participation in other MCSs. Since the depolarization-mediated reduction of cytosolic pH might have an impact on the affinity of PI(4)P for the effector proteins [176], pH measurements were necessary to be performed. Acidification of the cytosol was without effect on the cytosolic Ca<sup>2+</sup> concentration but caused drastic dissociation of OSBP from the Golgi. Depolarization stimulated the enrichment of OSBP on ISGs but this effect was abolished upon simultaneous alkalinization of the cytosol, indicating that the increase in cytosolic Ca<sup>2+</sup> concentration facilitate the association of OSBP with the ISGs partly through acidification. Interestingly, OSW-1 addition caused acidification of the cytosol in MIN6 cells, indicating putative additional effects of this drug in OSBP function distinct from its direct inhibitory action on the ORD domain.

### Coordination of OSBP and Sac2 on the surface of ISGs controls insulin secretion

OSBP has been previously reported as the major component of a ferry-bridge model that catalyzes the PI(4)P/cholesterol counter-exchange between the ER and TGN. Regulation of the levels of PI(4)P and cholesterol on the ISGs is indispensable for efficient insulin secretion [193, 257], and lack of Sac2 leads to excess accumulation of PI(4)P on the granular surface and to impaired insulin secretion [253, 258]. Staining of fixed MIN6 cells with the naturally fluorescent cholesterol marker filipin as well as the expression of the ISG marker NPY-mNG showed that ISGs are also rich in cholesterol. siRNA-mediated Sac2 knockdown resulted in strong accumulation of cholesterol in the membrane of ISGs. This indicated that PI(4)P might serve as the lipid form of ATP for the transport of cholesterol from the ER on the ISGs through the action of OSBP. Transient reduction of the OSBP expression resulted in slight reduction of the cholesterol levels in intracellular membranes. However, when OSBP and Sac2 expression was simultaneously reduced the excess cholesterol accumulation in ISG membranes was prevented. These results show the existence of an interplay between Sac2 and OSBP in order to regulate the ISG PI(4)P and cholesterol levels.

Since the ISG PI(4)P and cholesterol are two important regulators of insulin secretion, Sac2 and OSBP-dependent changes in insulin release were further explored. siRNA-mediated Sac2 or OSBP knockdown resulted in reduced insulin secretion upon depolarization or glucose stimulation. This was not accompanied by changes in the insulin content, indicating that the reduction in insulin secretion was the consequence of impaired insulin release and not

biogenesis. Similarly, acute inhibition of OSBP by OSW-1 suppressed both depolarization- and glucose-stimulated insulin secretion from MIN6 cells and mouse pancreatic islets, without markedly impacting the voltage-dependent  $\text{Ca}^{2+}$  influx. These results highlighted the role of OSBP and Sac2 for the lipid transport to ISGs to ensure normal insulin secretion, downstream the cargo loading process in the TGN.

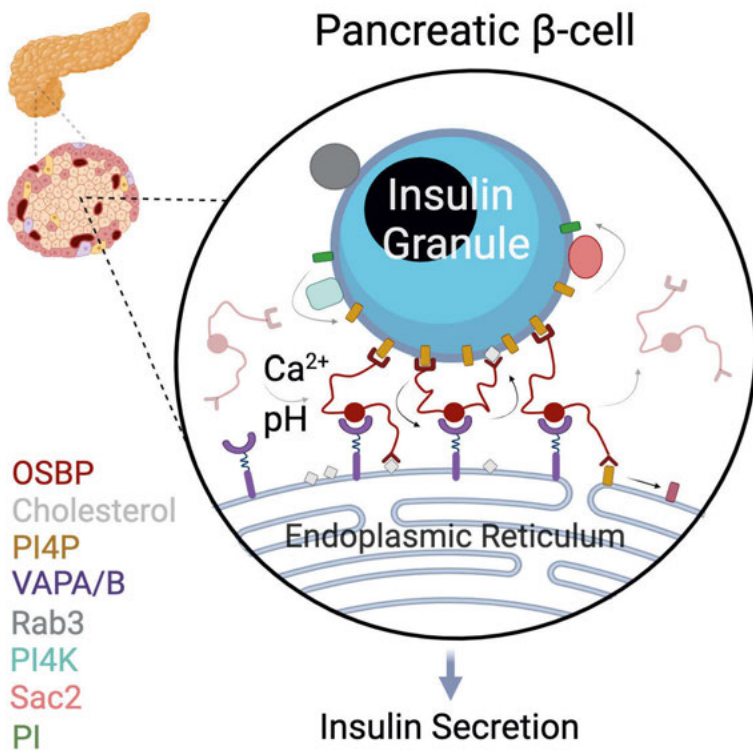


Figure 7: Cooperation between granule-localized Sac2 and OSBP controls the turnover of granular PI(4)P and counter-transport of cholesterol, respectively.

## Paper III

Mature ISGs can be classified into two distinct groups; the readily releasable pool (RRP) consisting of ISG located close to the PM and the reserve pool which is located deeper in the cytoplasm. The ISG release capacity upon stimulation is defined by the position, mobility and age of the ISGs, and is determined by the lipid and protein composition of the ISG membrane. Although the lipidomic and proteomic profile is established during the budding from the Golgi apparatus, there is growing evidence that membrane modifications can occur throughout the ISG lifetime. The alterations in the ISG membrane profile determines whether a granule is released or degraded, and both vesicular- and non-vesicular-based lipid transport likely contributes to ISG dynamics [12]. The negatively charged membrane of ISG in the early stages of the secretory pathway increases the release propensity of the granules as it allows the binding of effector proteins that facilitates microtubule-mediated transport to the PM. In the glucose-sensing  $\beta$  cells, the sugar uptake activates ATP production through glycolysis and oxidative phosphorylation. ATP is crucial for both the triggering and amplifying pathways of insulin secretion, but it is also stored in ISGs and co-released with insulin. It can act in an auto- or paracrine manner through purinergic receptors activation and downstream signalling [259]. Vesicular adenosine transporter (VNUT) is responsible for the ATP uptake and storage in the ISGs. Although the vesicular ATP accumulation is fuelled by the ISG membrane potential differences, the source of ATP and the exact mechanism of uptake is still unclear.

### TMEM24 is recruited to newly synthesized insulin granules

In paper I, we show that the presence of PI4-kinases on the surface of ISGs accounts partially for maintaining high levels of PI(4)P. In addition, the PI(4)P abundance on the ISG membrane can be regulated by the action of the PI(4)P-phosphatase Sac2 [253] and OSBP. Recent lipidomic analysis demonstrated the acidic phospholipids, phosphatidic acid (PA), phosphatidylserine (PS), and PI, mainly, contribute to the establishment of the negative charge on the membrane of younger ISGs. Therefore, we investigated if TMEM24, which transports PI and bind target membrane through interactions with negatively charged lipids [117], can act at the surface of ISGs during the maturation process.

Multi-labelling methodology coupled with pulse-chase protocols allowed us to distinguish younger (potentially immature) from older ISGs. More specifically, we fused the self-labelling protein HaloTag to the granular marker NPY (NPY-Halo) as it is designed to covalently bind a variety of synthetic ligands, thus enabling the visualization of temporally distinct ISGs. MIN6 cells overexpressing NPY-Halo and TMEM24-eGFP were incubated with JFX650 marking the preexisting ISG population (“Old Granules”). The

removal of the unbound ligand and high glucose conditions promoted the generation of new ISGs which were labelled with the spectrally separate ligand JFX549 (“New Granules”). In line with previous studies, under basal conditions TMEM24 was enriched at the plasma membrane and a small fraction was localized to the granules in the cytosolic area with no apparent preference over ISGs of a specific age. Depolarization-mediated  $\text{Ca}^{2+}$  influx, but not carbachol-induced ER  $\text{Ca}^{2+}$  efflux, revealed high enrichment of the PM-dissociated TMEM24 on the new ISGs in the cytosol, shortly after their budding from the trans-Golgi network (TGN).

### Time-dependent interactions between mitochondria and newly synthesized ISGs

In Paper I, we showed that  $\text{Ca}^{2+}$  influx triggered the redistribution of TMEM24 from the PM to mitochondria where it influenced the ATP production. In the current study, the same conditions triggered the recruitment of TMEM24 onto newly synthesized ISGs, suggesting a parallel proximity between mitochondria and ISGs. Immunolabeling of MIN6 cells expressing TMEM24-eGFP revealed the presence of mitochondria- and TMEM24-positive ISG subpopulation which doubled in number upon depolarization. In addition to that, we showed that the proximity between mitochondria and ISGs was time-dependent as mitochondria were observed in close proximity to new, but not old, ISGs. Confocal microscopy revealed a high degree of overlap between insulin and the outer-mitochondrial-membrane-localized voltage-dependent anion channel (VDAC). To overcome the resolution limit of the available light microscopes, Proximity ligation assay (PLA) was employed targeting the VDAC and the ISG marker Rab3. The proximity between the two markers allowed the generation of significant amount of detectable amplified PLA products compared the application of solely anti-VDAC. The mitochondria-ISG proximity was further supported by images retrieved from  $\beta$  cells in mouse pancreatic islets using high-resolution FIB-SEM, available through an open source (<https://openorganelle.janelia.org/>).

### Colocalization between VNUT and VDAC at newly synthesized ISGs

We hypothesized that the juxtaposition of the cell powerhouses and the insulin-loaded vesicles facilitate ATP transfer to the lumen of the latter. VNUT is a key element for vesicular ATP uptake and storage which is essential for normal insulin secretion. The overlap of the fluorescence signal from the insulin, VNUT and VDAC supported a scenario where VNUT/VDAC participates in mitochondria-ISG tethering. Moreover, VDAC was enriched on ISGs shortly after their departure from the Golgi. Following an orthogonal approach for the

visualization of newly synthesized granules, we applied a proinsulin trafficking reporter system based on the retention using selective hooks (RUSH) methodology [260, 261]. Streptavidin fused to an ER-retention sequence (KDEL) enables the confinement of the sfGFP-tagged proinsulin fused to a streptavidin-binding protein (SBP) inside the lumen of the ER (proCpepRUSH). Addition of biotin allows the release of proinsulin into the secretory pathway as biotin outcompetes the SBP streptavidin binding. This methodology allowed the synchronous export of ISG from the TGN increasing the chances to capture co-occurrence of transient events. Confocal images from islets expressing the proCpepRUSH system, 60 minutes after the addition of biotin, demonstrated high degree of overlap between RUSH-positive ISGs, VNUT and VDAC. However, this interaction was restricted to ISGs of a specific age, implying that VDAC and VNUT participate in ISGs-mitochondria interactions shortly after ISG formation. Since VNUT and VDAC are transmembrane proteins, a tethering molecule was next investigated. Mitofusin 2 (Mfn2) localizes in the outer mitochondrial membrane and promotes the tethering of mitochondria with other subcellular compartments, including the ER, peroxisomes and melanosomes [262-264]. Results from MIN6 cells as well as from mouse pancreatic islets expressing proCpepRUSH showed that Mfn2 colocalized with ISGs recently exited from the TGN that are also positive for VNUT, indicating that Mfn2 participates in the formation of mitochondria-ISG contacts.

### Reduced VNUT expression affects VDAC localization to newly synthesized ISGs and impairs ISG maturation

siRNA-mediated reduction of VNUT expression (VNUT KD) in MIN6  $\beta$ -cells abolished the overlap of the VNUT and VDAC fluorescence signal and, interestingly, also reduced the enrichment of VDAC on the RUSH-positive ISGs upon their export from the TGN. Since the formation of MCSs can affect both subcellular components, we investigated differences in the mitochondrial morphology in the VNUT KD cells. Although there were no apparent changes in the overall volume of the mitochondrial network, VNUT KD cells contained mitochondria with fewer and longer branches. In addition to morphological changes, we also found that the mitochondrial membrane potential was slightly increased in mitochondria in VNUT KD cells compared to control cells. These observations suggest that the VNUT-mediated ISG-mitochondria proximity might affect the mitochondrial structure and activity. Results from pulse chase and RUSH experiments revealed a reduction in the ratio of new to old granules, but no obvious impairment in granule exit from the TGN, in VNUT KD cells. These results indicate that VNUT plays a role in ISG maturation and/or turnover, but not biogenesis (Figure 8).

## Reduced VNUT expression impairs insulin secretion

Intracellular ATP is a key signalling molecule, coupling elevated glucose concentration to initiation of insulin release [265]. Extracellular ATP is a major contributor to the autocrine or paracrine regulation of  $\beta$ -cell function and the modulation of insulin secretion. Secreted ATP stimulates the  $G\alpha_q$  protein-dependent activation of phospholipase C (PLC) leading to the generation of inositol 1,4,5-trisphosphate ( $IP_3$ ), and diacylglycerol (DAG). We investigated the potential defects in ATP release in VNUT KD cells by expressing the mCherry-C1aC1b<sub>PKC</sub> in order to monitor changes in the levels of PM DAG [242] using TIRF microscopy. VNUT KD cells exhibited reduced ATP release and reduced number of ISG fusion events, reported by the pH-sensitive granule marker vesicle-associated membrane protein 2 (VAMP2)-pHluorin. The employment of a real-time optical assay based on the PH<sub>GRP1</sub>-GFP<sub>4</sub> which reports the generation of plasma membrane PI(3,4,5)<sub>3</sub> upon the activation of the insulin receptors [266] confirmed reduced insulin secretion in VNUT KD cells. Collectively, VNUT expression is essential for the successful ISG exocytosis.

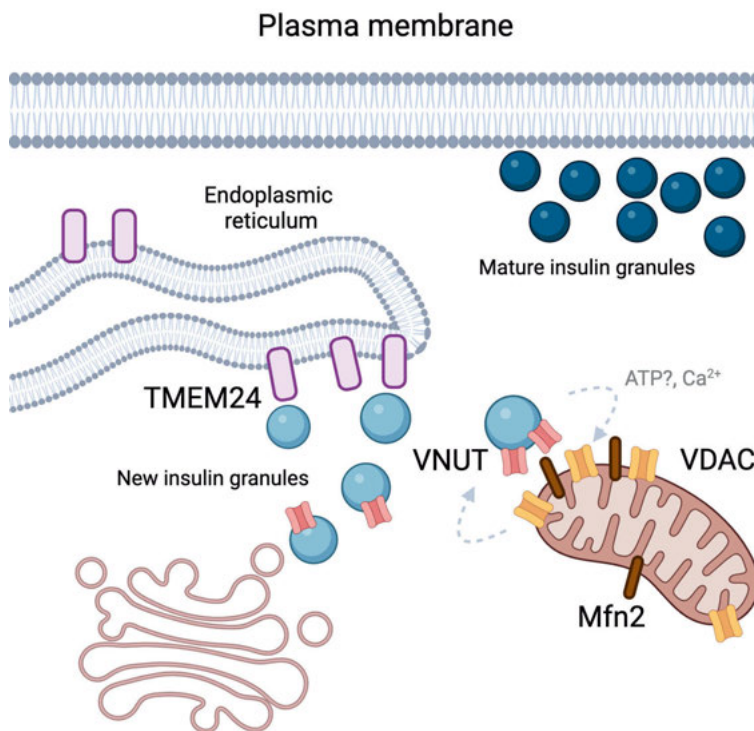


Figure 8: Insulin granules associate with ER-anchored TMEM24 and VDAC- and Mfn2-enriched mitochondria regions during the maturation process.



# Conclusions

- I. In study I, we show that ER-anchored TMEM24 dissociates from the plasma membrane in response to elevated cytosolic  $\text{Ca}^{2+}$  and instead make contact with mitochondria. TMEM24 knockout cells presented with depolarized mitochondria that hyperaccumulated  $\text{Ca}^{2+}$  and exhibited impaired glucose-stimulated ATP production, which in turn led to impaired sustained insulin secretion. These results suggest that TMEM24 influence mitochondrial function directly, either by controlling the transfer of  $\text{Ca}^{2+}$  between to or from the ER or by modulating the activity of other protein located at ER-mitochondria contacts.
- II. In study II, we show that oxysterol-binding protein (OSBP) plays a vital role in the regulation of insulin secretion through its involvement in lipid exchange at ER-ISG contact sites. Glucose-induced increase in  $\text{Ca}^{2+}$  levels and subsequent acidification enhanced the interactions between OSBP and ISG, which were essential for normal insulin secretion. Mechanistically, we show that OSBP controls cholesterol transfer to the ISG membrane where it works in conjunction with the granule-localized PI(4)P phosphatase Sac2. Although OSBP interacts with granules at these contact sites, it does not appear to be involved in contact site formation, indicating that its primary function is to facilitate lipid exchange and not to establish physical connections.
- III. In study III, we revealed significant interactions occurring between ISGs and both ER and mitochondria shortly after granule formation at the Golgi, and show that ER-localized TMEM24, granule-localized VNUT and mitochondria-localized VDAC and Mfn2 define these sites. Reduction of VNUT expression abolishes the ISG-mitochondria interaction and resulted in reduced ATP accumulation in ISGs and in impaired insulin secretion.

## Future Perspectives

As this research demonstrates the importance of membrane contact sites for the function of  $\beta$  cells, it has also unveiled several intriguing gaps that warrant further investigation. Although contact sites formed between the ER and the ISGs represent a PI(4)P/cholesterol exchange platform, additional reactions might occur between the opposed membranes of these two organelles. The exploration of these mechanisms as well as their regulatory effectors would benefit from the identification of the exact tethering and regulatory components involved in the formation of ER-ISG contacts.

Using tools that enable the contact-dependent proximity labelling in cells will enable mapping of the endogenous proteome of the ER-ISG contact sites. The proximity labelling techniques originally consisted of promiscuous enzymes such as APEX [267, 268], BioID [269] or TurboID [270] to target the protein of interest. The addition of biotin-derived molecules will allow the biotinylation of the surrounding proteins. Upon cell lysis, biotinylated proteins can be harvested with streptavidin-coated beads and can be further identified by mass spectrometry. However, in my studies spatial specificity is essential. To achieve this, split variants of the enzymes above are better tool candidates. Therefore, fusing the two fragments on proteins that participate in the formation of ER-ISGs will restrict the biotinylation activity to the contact site. Compared to the split versions of APEX [271] and BioID [272-274], split-TurboID does not require any cofactors or co-oxidants besides biotin and it is >100-fold faster than BioID since the labelling time is 1 to 10 min [270]. So far, I have fused the two fragments of Split-TurboID on ER-located Sec61b and the IG-transmembrane protein phogrin (Figure 9A), and I have assessed the specificity of the assay using fluorescent microscopy. More specifically, I transfected MIN6 cells with the Split-TurboID- containing plasmids along with an IG marker (NPY-mNGr) and allowed the system to be expressed for 48h before fixation. To visualize the system, I incubated my samples with fluorescent-conjugated streptavidin. From my preliminary data (Figure 9B), the signal from the Split-TurboID highly overlaps with the IG marker. However, there is high background noise from endogenously biotinylated proteins which needs to be further optimized. Since the proteome analysis requires large amounts of cell lysates, the generation of a cell line stably expressing the system is necessary. This will allow the downstream proteome analysis of the ER-ISG contact sites using mass spectrometry.

Metabolic stress due to obesity and hyperglycaemia can cause ER stress as well as activation of the unfolded protein response (UPR) [275]. Failure of the UPR to restore the ER homeostasis can lead to  $\beta$ -cell malfunction in T1D and T2D [276, 277]. It would be intriguing to examine how the ER-ISG MCSs behave under ER-stress-inducing conditions using high-resolution microscopy or the proximity ligation assay, and complement the data with observations acquired from donors with T1D and T2D.

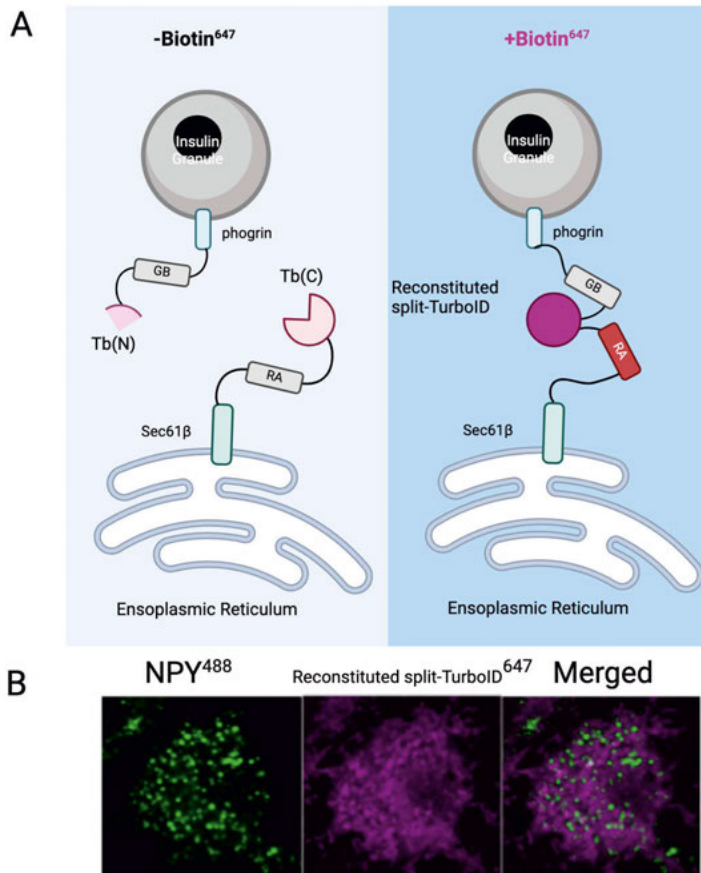


Figure 9: A. Schematic overview of the Split-TurboID assay targeting the contact sites of ER and ISGs. B. MIN6 cell transiently expressing the ISG marker NPY-mNGreen and the Split-TurboID fragments TB(C) and Tb(N) fused to ER (Sec61 $\beta$ ) - and ISG (phogrin)- localized proteins, respectively. Addition of biotin catalyses the reconstitution of the split-TurboID molecule

The establishment of a MIN6 cell line stably expressing the ER-ISG contact site reporter (RA-Sec61 $\beta$ /GB-Rab3a) will also allow us to perform studies on the dynamic changes of the contact sites in living cells under various physiological and pathophysiological conditions, such as different glucose

concentrations, amino acids and fatty acids as well as under conditions of ER stress. However, there are no standardized ways to quantify the contact sites. Therefore, we will explore potential image analysis methods that will allow us to understand better the structure and function of the reconstituted ER-ISG MCSs. The investigation will be extended to mouse and human pancreatic islets. For this purpose, the generation of an adenovirus carrying the reporter system (Ad-EF1a-RA-Sec61b-IRES-GB-Rab3) is essential so we can efficiently infect the primary  $\beta$  cells and enable visualization of ER-ISG contact sites.

Furthermore, the data from the last study suggest that new insulin granules can have direct impact on the  $\beta$  cell metabolism through crosstalk with mitochondria. This shows that the reserve pool of insulin granules is not only an energy source downstream of degradation but can also actively influence mitochondrial function. However, if the exact mechanism involves ion or lipid transport is still unknown. Preliminary data using PLA, showed that VNUT on the granule surface interacts with VDAC1 on mitochondria (Figure 10). VDAC1 is differentially expressed in T2D [278] and it will be important to determine how potential changes in ER-ISG contacts contributes to pathological changes in the  $\beta$  cells.

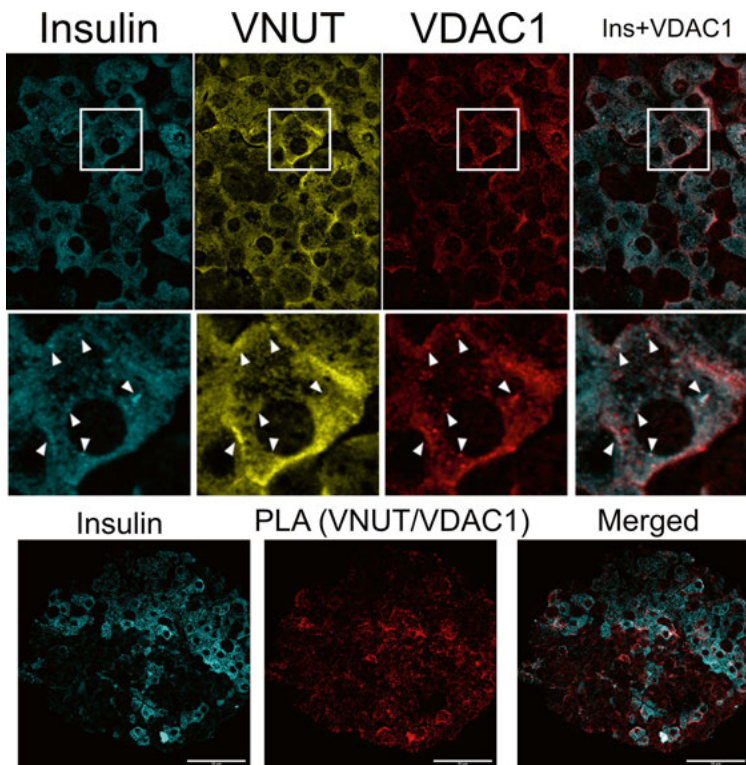


Figure 10: Immunofluorescence against insulin, VNUT and VDAC1 (upper panels) and PLA using antibodies against VNUT and VVDAC1 and downstream immunofluorescence against insulin (lower panel)

# Περίληψη

**Τίτλος διδακτορικής διατριβής:** Ενδοεπικοινωνία των οργανιδίων στα β παγκρεατικά κύτταρα: Τα σημεία επαφής των μεμβρανών μεταξύ των οργανιδίων ως ρυθμιστές της έκκρισης ινσουλίνης

**Εισαγωγή:** Σήμερα γνωρίζουμε ότι τα οργανίδια του κυττάρου δεν δρουν αποκλειστικά ως αυτόνομες δομές αλλά είναι συντελεστές ενός καλά ρυθμισμένου δικτύου κι αυτό διότι μπορούν να έρχονται σε πολλή μικρή απόσταση μεταξύ τους, στα σημεία επαφής των μεμβρανών (ΣΕΜ). Τα σημεία αυτά λειτουργούν ως πλατφόρμες που διευκολύνουν την αλληλεπίδραση των οργανιδίων. Πιο συγκεκριμένα, τα ΣΕΜ επιτρέπουν την μεταφορά ασβεστίου και λιπιδίων τα οποία παίζουν πολύ σημαντικό ρόλο για την εύρυθμη λειτουργία των οργανιδίων και κατ' επέκταση ολόκληρου του κυττάρου. Η μεταφορά των διαφόρων υλικών καταλύεται, σε ορισμένες περιπτώσεις, από πρωτεΐνες-μεταφορείς των λιπιδίων (ΠΜΛ). Η παρούσα διπλωματική εστιάζει στο πως τα ΣΕΜ επηρεάζουν την λειτουργία των β παγκρεατικών κυττάρων, τα οποία είναι ο πολυπληθέστερος τύπος ενδοκρινών κυττάρων των παγκρεατικών νησίδων του Langerhans, υπεύθυνα για την έκκριση της ινσουλίνης. Το «ταξίδι» της ινσουλίνης στο κύτταρο ξεκινάει στο ενδοπλασματικό δίκτυο, με τη σύνθεση του πρόδρομου μορίου της προ-προϊνσουλίνης, η οποία με περαιτέρω επεξεργασία μέσα στο δίκτυο Golgi μετατρέπεται σε προϊνσουλίνη και εισάγεται μαζί με άλλα μόρια μέσα σε πρώιμα κυστίδια ινσουλίνης που ξεπροβάλλουν από το δίκτυο Golgi. Τα κυστίδια αυτά μεταφέρονται κοντά στην πλασματική μεμβράνη (ΠΜ), όπου μετά την αύξηση της συγκέντρωσης του ασβεστίου στον ενδοκυτταρικό χώρο (π.χ. όταν ανιχνεύεται υψηλή γλυκόζη στο αίμα), διάφορα ένζυμα στο εσωτερικό των κυστιδίων συμβάλλουν στην ωρίμαση της προϊνσουλίνης σε ινσουλίνη, η οποία απελευθερώνεται στην κυκλοφορία του αίματος. Η επιτυχία στη διαδικασία έκκρισης της ινσουλίνης εξαρτάται από πολλούς παράγοντες: τη σύνθεση του μορίου, τη φόρτωση του στα κυστίδια μαζί με τα άλλα μόρια, τη μεταφορά των κυστιδίων μέσω του κυτταροσκελετού στην πλασματική μεμβράνη, τη σύζευξη των κυστιδίων με την πλασματική μεμβράνη και το άδειασμα του περιεχομένου των κυστιδίων στον εξωκυτταρικό χώρο. Κομβικό ρόλο σε όλες αυτές τις διαδικασίες παίζει η πρωτεϊνική και λιπιδική σύνθεση των μεμβρανών των κυστιδίων ινσουλίνης (ΚΙ). Η σύσταση αυτή αλλάζει καθ' όλη τη διάρκεια του ταξιδιού των ΚΙ μέσα

στο κύτταρο, γεγονός που υποδεικνύει ότι η ταυτότητα της μεμβράνης των κυστιδίων δεν καθορίζεται αποκλειστικά από την αφετηρία δημιουργίας τους (δίκτυο Golgi), αλλά μπορεί να μεταβάλλεται κατά την αλληλεπίδραση των ΚΙ με τα υπόλοιπα κυτταρικά οργανίδια στα ΣΕΜ.

Παρακάτω συνοψίζονται τα σημαντικότερα ευρήματα των μελετών της διδακτορικής διατριβής:

**Άρθρο I:** Σε αυτό το άρθρο εστίασαμε στο TMEM24, μία ΠΜΛ η οποία είναι πάνω στο ενδοπλασματικό δίκτυο (ΕΔ) και ρόλος της είναι να μεταφέρει φωσφατιδυλοϊνοσιτόλη από το ΕΔ στην ΠΜ σε συγκεκριμένα ΣΕΜ. Η φωσφατιδυλοϊνοσιτόλη και τα παράγωγα της επηρεάζουν άμεσα πολλά σηματοδοτικά μονοπάτια στην ΠΜ τα οποία είναι σημαντικά για την έκκριση της ινσουλίνης. Στην παρούσα έρευνα μας, βρήκαμε ότι η θέση του TMEM24, εξαρτάται άμεσα από τα επίπεδα ενδοκυτταρικού ασβεστίου και διακυλογλυκερόλης, τα οποία όταν αυξάνονται, το TMEM24 απομακρύνεται από την ΠΜ και γίνεται διαθέσιμο σε σημεία κοντά στα μιτοχόνδρια. Η απώλεια του TMEM24 προκάλεσε συσσώρευση ασβεστίου στο ΕΔ και τα μιτοχόνδρια, μεταβάλλοντας το δυναμικό της μεμβράνης των μιτοχονδρίων, γεγονός που επιδρά αρνητικά στην παραγωγή ενέργειας από τα συγκεκριμένα οργανίδια και κατ' επέκταση στην έκκριση ινσουλίνης.

**Άρθρο II:** Σε αυτή τη μελέτη εντοπίσαμε για πρώτη φορά την ύπαρξη ΣΕΜ μεταξύ του ΕΔ και των ΚΙ. Για το σκοπό αυτό χρησιμοποιήσαμε τεχνικές μικροσκοπίας υψηλής ανάλυσης καθώς και μεθοδολογίες που μας επέτρεψαν να παρατηρήσουμε τις συγκεκριμένες ΣΕΜ στο χώρο και στο χρόνο. Εντοπίσαμε, επίσης πως σε αυτές τις ΣΕΜ, σημαντικό ρόλο έχει η OSBP, μία ΠΜΛ η οποία έχει την ικανότητα να ανταλλάσσει χοληστερόλη με PI(4) (παράγωγο της φωσφατιδυλοϊνοσιτόλης). Σε συνθήκες ηρεμίας, η OSBP, βρίσκεται στις ΣΕΜ μεταξύ του ΕΔ και του δικτύου Golgi. Ωστόσο, όταν μπλοκάρουμε την ικανότητα της OSBP να ανταλλάσσει λιπίδια, το μόριο αυτό αλλάζει θέση και συγκεντρώνεται σε περιοχές πλησίον των ΚΙ. Σύμφωνα με τα αποτελέσματά μας, η εύρυθμη λειτουργία της OSBP καθώς και η σωστή συνεργασία του με άλλα ένζυμα πάνω στα ΚΙ για τη ρύθμιση των επιπέδων της χοληστερόλης στη μεμβράνη των ΚΙ είναι απαραίτητα για αποτελεσματική έκκριση ινσουλίνης.

**Άρθρο III:** Σε αυτό το άρθρο εστίασαμε στους δύο διαφορετικούς υποπληθυσμούς των ΚΙ βάσει της ηλικίας τους. Χρησιμοποιώντας τα κατάλληλα μοριακά εργαλεία και συνεστιακή μικροσκοπία, παρατηρήσαμε ότι τα νέα ΚΙ, δηλαδή τα ΚΙ που πρόσφατα εξήχθησαν από το δίκτυο Golgi έρχονται σε μικρή απόσταση με το TMEM24, το οποίο μελετήσαμε στο άρθρο I, όταν υπάρχει αύξηση του ενδοκυτταρικού ασβεστίου. Επίσης παρατηρήθηκε, για πρώτη φορά, ότι τα νέα ΚΙ έρχονται σε επαφή με τα μιτοχόνδρια σε σημεία

που συγκεντρώνεται στη εξωτερική μεμβράνη των μιτοχονδρίων το κανάλι για τη μεταφορά ασβεστίου και άλλων μικρών μορίων καθώς και συνδεδετικά μόρια που συμμετέχουν σε άλλα παραδοσιακά είδη ΣΕΜ. Παρατηρήθηκε ότι η επαφή με τα μιτοχόνδρια είναι απαραίτητη για την αποτελεσματική δημιουργία των ΚΙ. Ωστόσο δε γνωρίζουμε ακόμη τον ακριβή μηχανισμό και τη μεταφορά ποιου/ων μορίου/ων εξυπηρετεί.

# Acknowledgements

*“The totality is not, as it were, a mere heap, but the whole is something besides the parts”*

*Aristotle’s Metaphysics, Book VIII, 1045a.8–10.*

The work presented in this thesis was performed in the Department of Medical Cell Biology, Uppsala University, with support from the Swedish Research Council, Diabetesfonden, Stiftelsen familjen Ernfors fond and EXODIAB.

I would like to express my sincere gratitude to all the people that supported me during this challenging academic and personal journey.

First, I would like to express my deepest gratitude to **Olof Idevall-Hagren**, my supervisor, for his unwavering support, guidance, and encouragement all these years. Your optimism and dedication have been a source of constant inspiration, and your insightful feedback has greatly enriched my work. Your patience, availability, and willingness to help at every stage of my studies have made a significant impact, allowing me to overcome challenges and grow both academically and personally. I am truly fortunate to have had the privilege of working under your mentorship, and I will always carry the lessons learned during this time with immense gratitude. Thank you for being the perfect balance to the chaos I had sometimes in my head, for reminding me to slow down when I was close to burnout, calming me down when I was panicking and pointing out the bright side of things when I was desperately negative.

I extend my heartfelt gratitude to my co-supervisor, **Anders Tengholm**, for his invaluable feedback and guidance throughout this journey. Your vast experience and expertise in the islet physiology have been instrumental in shaping the direction and depth of my work. Your approachable nature and willingness to share your profound knowledge have been a source of inspiration and learning.

**Johan Kreuger**, my co-supervisor, thank you for your commitment to ensuring that everything ran smoothly throughout my research journey.



To all my former and current colleagues of the “Idevall-Tengholm” research groups, who have made this journey an unforgettable experience with their collaboration but most importantly their friendship, trust and mutual support.

**Kia Wee**, I am deeply grateful to you for your guidance and support throughout my research. Working closely with you was an invaluable learning experience. Your kindness, patience, and unwavering belief in my abilities have meant more to me than words can express, and I am truly fortunate to have had you as both a mentor and a friend. Your friendship has been a true gift, I will always cherish our moments in and out of the lab, the laughter, the discussions, even working together until 11 pm.

**Gonzalo**, thank you for all our beautiful, unstructured, long fikas. **Ylva, Moa, Kousik**, my lovely chickens, I feel the luckiest person on earth working by your side. You bring so much joy in the lab, making it a place I was looking forward to come back the following day. **Bryon**, thank you for making sure I always have enough amount of chocolate. **Yunjian**, it was a pleasure sharing the office with you, I apologize for the amount of perfume I was wearing some days. **Oleg**, I will miss your deep voice saying “Hello Stela” every day, and I would also like to thank you for your insightful feedback to my work, our broad-spectrum discussions and for providing me with the delicious Paska every Easter. **Mingyu**, thank you for your great company all these years. **Helene and Erik**, it was an honor working with you. **Beichen**, thank you for inspiring me to pursue this PhD, I really enjoyed working with you and I am excited every time I get to meet you in the conferences.

I am deeply grateful to my dear friend, **Maria Kopsida**, for being a constant source of support and encouragement. You made the experience much richer and more meaningful. Your advice, your ability to make me laugh, keep things in perspective, and offer a listening ear has meant the world to me. I am incredibly fortunate to have met you.

To all former and current PhD students in the MCB, especially **Maja, Christina, Ada, Marie, Santiago, Liangwen, Lina, Casian, Julia, Quan**, I had a great time with you guys, meeting you in the corridors, having lunch and fikas with you. Thank you for being the dose of laughter that kept me going throughout the day.

To my dearest neighbours, **Rajni and Sagho**, I’m beyond grateful for your company, I have laughed with all my heart during our time together. Thank you for keeping me fed and being an important part of this journey. I will always cherish our moments.

Ανιψούλες μου, **Λένια** και **Αναστασία**, σας ευχαριστώ που ήσασαν μία αστείρευτη πηγή γέλιου. **Βασίλη** και **Σοφία**, ευχαριστώ για όλη την αγάπη, τη φροντίδα, την ψυχολογική υποστήριξη, την εμπύχωση, τις αστείες (βιντεο)κλήσεις όλα αυτά τα χρόνια.

Κυρία **Εύα** και κύριε **Πύρρο**, ευχαριστώ για όλη την αγάπη σας, την περιποίηση και την ζεστή υποδοχή στην οικογένεια σας.

Ευχαριστώ τις **γιαγιάδες** και τον **παπού** μου για τη στοργή τους και το ξεμάτιασμα, τα **ξαδέρφια** και τους **θείους** μου για τα γέλια μέσω του «ομορφόσογου» αλλά και όποτε ήμουν «σπίτι».

Στο **Μαράκι** μου, «α την ευχαριστήσε πολύ της λέει», που πάντα την άκουγε και όταν δεν την άκουγε «τα άκουγε».

**Θοδωρή** μου, αγάπη μου, τίποτα δε θα μπορούσε να έχει γίνει χωρίς εσένα. Η αγάπη σου, η ηθική και συναισθηματική σου υποστήριξη μου έδινε καθημερινά δύναμη να συνεχίζω. Σ' ευχαριστώ που ήσουν εκεί στα δύσκολα και στα ευχάριστα όλα αυτά τα χρόνια.

Στο διδυμάκι μου, **Μαρία**, ένα «ευχαριστώ» είναι πολύ λίγο. Ρουλινάκο μου, ήσουν πάντα εκεί να με ακούσεις όταν γκρίνιαζα ή έκλαιγα ή και τα δύο μαζί, πάντα να με εμπυχώνεις και να μου λες πως θα τα καταφέρω. Στο **Αλμπουσινάκι** και το **Μινερβίνι**, ευχαριστώ για την τσάμπα ψυχοθεραπεία και τον πιο ξεκούραστο ύπνο.

Οι πιο εγκάρδιες και θερμές ευχαριστίες μου πάνε στους γονείς μου, **Έλενα** και **Δημήτρη**. Μανουλάκι και Μπαμπινάκο, χωρίς τη στήριξη σας δε θα τα είχα καταφέρει. Σας ευχαριστώ που είστε πάντα δίπλα μου, με ενθαρρύνετε να πραγματοποιώ τα όνειρά μου, πιστεύετε σε εμένα και με οπλίζατε με θάρρος και δύναμη να καταφέρω κάτι τόσο μεγάλο. Η υπομονή, η κατανόηση, η αγάπη, η συνεχής σας παρουσία με έκαναν να αισθάνομαι πως δεν είμαι μόνη σε όλο αυτό αλλά είμαι «πρώωώώωτη».

# References

1. Da Silva Xavier, G., *The Cells of the Islets of Langerhans*. J Clin Med, 2018. **7**(3).
2. Fu, Z., E.R. Gilbert, and D. Liu, *Regulation of insulin synthesis and secretion and pancreatic Beta-cell dysfunction in diabetes*. Curr Diabetes Rev, 2013. **9**(1): p. 25-53.
3. Fazakerley, D.J., et al., *Muscle and adipose tissue insulin resistance: malady without mechanism?* J Lipid Res, 2019. **60**(10): p. 1720-1732.
4. Briant, L., et al., *Glucagon secretion from pancreatic  $\alpha$ -cells*. Ups J Med Sci, 2016. **121**(2): p. 113-9.
5. Brazeau, P., et al., *Hypothalamic polypeptide that inhibits the secretion of immunoreactive pituitary growth hormone*. Science, 1973. **179**(4068): p. 77-9.
6. Rorsman, P. and M.O. Huising, *The somatostatin-secreting pancreatic  $\delta$ -cell in health and disease*. Nat Rev Endocrinol, 2018. **14**(7): p. 404-414.
7. Nolan, C.J., P. Damm, and M. Prentki, *Type 2 diabetes across generations: from pathophysiology to prevention and management*. Lancet, 2011. **378**(9786): p. 169-81.
8. Kahn, S.E., *Clinical review 135: The importance of beta-cell failure in the development and progression of type 2 diabetes*. J Clin Endocrinol Metab, 2001. **86**(9): p. 4047-58.
9. Marchetti, P., et al., *The pancreatic beta-cell in human Type 2 diabetes*. Nutr Metab Cardiovasc Dis, 2006. **16 Suppl 1**: p. S3-6.
10. Colagiuri, S., *Diabesity: therapeutic options*. Diabetes Obes Metab, 2010. **12**(6): p. 463-73.
11. McGarry, J.D., *Banting lecture 2001: dysregulation of fatty acid metabolism in the etiology of type 2 diabetes*. Diabetes, 2002. **51**(1): p. 7-18.
12. Omar-Hmeadi, M. and O. Idevall-Hagren, *Insulin granule biogenesis and exocytosis*. Cell Mol Life Sci, 2021. **78**(5): p. 1957-1970.
13. Müller, A., et al., *3D FIB-SEM reconstruction of microtubule-organelle interaction in whole primary mouse  $\beta$  cells*. J Cell Biol, 2021. **220**(2).
14. Zhao, Y., et al., *Rapid structural change in synaptosomal-associated protein 25 (SNAP25) precedes the fusion of single vesicles with the plasma membrane in live chromaffin cells*. Proc Natl Acad Sci U S A, 2013. **110**(35): p. 14249-54.
15. Dodson, G. and D. Steiner, *The role of assembly in insulin's biosynthesis*. Curr Opin Struct Biol, 1998. **8**(2): p. 189-94.
16. Patzelt, C., et al., *Detection and kinetic behavior of preproinsulin in pancreatic islets*. Proc Natl Acad Sci U S A, 1978. **75**(3): p. 1260-4.
17. Huang, X.F. and P. Arvan, *Intracellular transport of proinsulin in pancreatic beta-cells. Structural maturation probed by disulfide accessibility*. J Biol Chem, 1995. **270**(35): p. 20417-23.
18. Olsen, H.L., et al., *Phosphatidylinositol 4-kinase serves as a metabolic sensor and regulates priming of secretory granules in pancreatic beta cells*. Proc Natl Acad Sci U S A, 2003. **100**(9): p. 5187-92.

19. Mesmin, B., B. Antonny, and G. Drin, *Insights into the mechanisms of sterol transport between organelles*. Cell Mol Life Sci, 2013. **70**(18): p. 3405-21.
20. Mesmin, B., et al., *Sterol transfer, PI4P consumption, and control of membrane lipid order by endogenous OSBP*. Embo j, 2017. **36**(21): p. 3156-3174.
21. Tarling, E.J., T.Q. de Aguiar Vallim, and P.A. Edwards, *Role of ABC transporters in lipid transport and human disease*. Trends Endocrinol Metab, 2013. **24**(7): p. 342-50.
22. Davidson, H.W., C.J. Rhodes, and J.C. Hutton, *Intraorganellar calcium and pH control proinsulin cleavage in the pancreatic beta cell via two distinct site-specific endopeptidases*. Nature, 1988. **333**(6168): p. 93-6.
23. Orci, L., et al., *Conversion of proinsulin to insulin occurs coordinately with acidification of maturing secretory vesicles*. J Cell Biol, 1986. **103**(6 Pt 1): p. 2273-81.
24. Arous, C. and P.A. Halban, *The skeleton in the closet: actin cytoskeletal remodeling in  $\beta$ -cell function*. Am J Physiol Endocrinol Metab, 2015. **309**(7): p. E611-20.
25. Wang, Z. and D.C. Thurmond, *Mechanisms of biphasic insulin-granule exocytosis - roles of the cytoskeleton, small GTPases and SNARE proteins*. J Cell Sci, 2009. **122**(Pt 7): p. 893-903.
26. Yasuda, T., et al., *Rim2alpha determines docking and priming states in insulin granule exocytosis*. Cell Metab, 2010. **12**(2): p. 117-29.
27. Barg, S., et al., *A subset of 50 secretory granules in close contact with L-type  $Ca^{2+}$  channels accounts for first-phase insulin secretion in mouse beta-cells*. Diabetes, 2002. **51 Suppl 1**: p. S74-82.
28. Thorn, P., et al., *Exocytosis in non-neuronal cells*. J Neurochem, 2016. **137**(6): p. 849-59.
29. Xu, T., et al., *Inhibition of SNARE complex assembly differentially affects kinetic components of exocytosis*. Cell, 1999. **99**(7): p. 713-22.
30. Jockusch, W.J., et al., *CAPS-1 and CAPS-2 are essential synaptic vesicle priming proteins*. Cell, 2007. **131**(4): p. 796-808.
31. Baker, R.W., et al., *A direct role for the Sec1/Munc18-family protein Vps33 as a template for SNARE assembly*. Science, 2015. **349**(6252): p. 1111-4.
32. Wang, S., et al., *Munc18 and Munc13 serve as a functional template to orchestrate neuronal SNARE complex assembly*. Nat Commun, 2019. **10**(1): p. 69.
33. Pinheiro, P.S., et al., *Doc2b synchronizes secretion from chromaffin cells by stimulating fast and inhibiting sustained release*. J Neurosci, 2013. **33**(42): p. 16459-70.
34. Barg, S., et al., *Fast exocytosis with few  $Ca(2+)$  channels in insulin-secreting mouse pancreatic B cells*. Biophys J, 2001. **81**(6): p. 3308-23.
35. Rorsman, P. and E. Renström, *Insulin granule dynamics in pancreatic beta cells*. Diabetologia, 2003. **46**(8): p. 1029-45.
36. Straub, S.G. and G.W. Sharp, *Glucose-stimulated signaling pathways in biphasic insulin secretion*. Diabetes Metab Res Rev, 2002. **18**(6): p. 451-63.
37. Henquin, J.C. and H.P. Meissner, *Effects of amino acids on membrane potential and  $86Rb^{+}$  fluxes in pancreatic beta-cells*. Am J Physiol, 1981. **240**(3): p. E245-52.
38. Cen, J., E. Sargsyan, and P. Bergsten, *Fatty acids stimulate insulin secretion from human pancreatic islets at fasting glucose concentrations via mitochondria-dependent and -independent mechanisms*. Nutr Metab (Lond), 2016. **13**(1): p. 59.

39. Cook, D.L., W.E. Crill, and D. Porte, Jr., *Glucose and acetylcholine have different effects on the plateau pacemaker of pancreatic islet cells*. *Diabetes*, 1981. **30**(7): p. 558-61.
40. Lewandowski, S.L., et al., *Pyruvate Kinase Controls Signal Strength in the Insulin Secretory Pathway*. *Cell Metab*, 2020. **32**(5): p. 736-750.e5.
41. Ashcroft, F.M. and P. Rorsman, *Electrophysiology of the pancreatic beta-cell*. *Prog Biophys Mol Biol*, 1989. **54**(2): p. 87-143.
42. Norris, N., B. Yau, and M.A. Kebede, *Isolation and Proteomics of the Insulin Secretory Granule*. *Metabolites*, 2021. **11**(5).
43. Kasai, H., et al., *Exocytosis in Islet  $\beta$ -Cells*, in *The Islets of Langerhans*, M.S. Islam, Editor. 2010, Springer Netherlands: Dordrecht. p. 305-338.
44. Ohara-Imaizumi, M., et al., *Imaging analysis reveals mechanistic differences between first- and second-phase insulin exocytosis*. *J Cell Biol*, 2007. **177**(4): p. 695-705.
45. Barg, S., et al., *Delay between fusion pore opening and peptide release from large dense-core vesicles in neuroendocrine cells*. *Neuron*, 2002. **33**(2): p. 287-99.
46. Pedersen, M.G. and A. Sherman, *Newcomer insulin secretory granules as a highly calcium-sensitive pool*. *Proc Natl Acad Sci U S A*, 2009. **106**(18): p. 7432-6.
47. Martens, G.A., *Species-Related Differences in the Proteome of Rat and Human Pancreatic Beta Cells*. *J Diabetes Res*, 2015. **2015**: p. 549818.
48. Hoboth, P., et al., *Aged insulin granules display reduced microtubule-dependent mobility and are disposed within actin-positive multigranular bodies*. *Proc Natl Acad Sci U S A*, 2015. **112**(7): p. E667-76.
49. Ivanova, A., et al., *Age-Dependent Labeling and Imaging of Insulin Secretory Granules*. *Diabetes*, 2013. **62**(11): p. 3687-3696.
50. Yau, B., et al., *A fluorescent timer reporter enables sorting of insulin secretory granules by age*. *Journal of Biological Chemistry*, 2020. **295**(27): p. 8901-8911.
51. Ohara-Imaizumi, M., et al., *TIRF imaging of docking and fusion of single insulin granule motion in primary rat pancreatic beta-cells: different behaviour of granule motion between normal and Goto-Kakizaki diabetic rat beta-cells*. *Biochem J*, 2004. **381**(Pt 1): p. 13-8.
52. Shibasaki, T., et al., *Essential role of Epac2/Rap1 signaling in regulation of insulin granule dynamics by cAMP*. *Proc Natl Acad Sci U S A*, 2007. **104**(49): p. 19333-8.
53. Schatz, H., C. Nierle, and E.F. Pfeiffer, *(Pro-) insulin biosynthesis and release of newly synthesized (pro-) insulin from isolated islets of rat pancreas in the presence of amino acids and sulphonylureas*. *Eur J Clin Invest*, 1975. **5**(6): p. 477-85.
54. Gold, G., M.L. Gishizky, and G.M. Grodsky, *Evidence that glucose "marks" beta cells resulting in preferential release of newly synthesized insulin*. *Science*, 1982. **218**(4567): p. 56-8.
55. Rhodes, C.J. and P.A. Halban, *Newly synthesized proinsulin/insulin and stored insulin are released from pancreatic B cells predominantly via a regulated, rather than a constitutive, pathway*. *J Cell Biol*, 1987. **105**(1): p. 145-53.
56. Balch, W.E., et al., *Vesicular stomatitis virus glycoprotein is sorted and concentrated during export from the endoplasmic reticulum*. *Cell*, 1994. **76**(5): p. 841-52.
57. Barclay, J.W., et al., *Phosphorylation of Munc18 by protein kinase C regulates the kinetics of exocytosis*. *J Biol Chem*, 2003. **278**(12): p. 10538-45.

58. Hou, J.C., L. Min, and J.E. Pessin, *Insulin granule biogenesis, trafficking and exocytosis*. Vitam Horm, 2009. **80**: p. 473-506.
59. Brunner, Y., et al., *Proteomics analysis of insulin secretory granules*. Mol Cell Proteomics, 2007. **6**(6): p. 1007-17.
60. Hickey, A.J., et al., *Proteins associated with immunopurified granules from a model pancreatic islet beta-cell system: proteomic snapshot of an endocrine secretory granule*. J Proteome Res, 2009. **8**(1): p. 178-86.
61. Schwartz, D., et al., *Improved characterization of the insulin secretory granule proteomes*. J Proteomics, 2012. **75**(15): p. 4620-31.
62. Suckale, J. and M. Solimena, *The insulin secretory granule as a signaling hub*. Trends Endocrinol Metab, 2010. **21**(10): p. 599-609.
63. Thomas-Reetz, A., et al., *A gamma-aminobutyric acid transporter driven by a proton pump is present in synaptic-like microvesicles of pancreatic beta cells*. Proc Natl Acad Sci U S A, 1993. **90**(11): p. 5317-21.
64. Walch-Solimena, C., et al., *Synaptotagmin: a membrane constituent of neuropeptide-containing large dense-core vesicles*. J Neurosci, 1993. **13**(9): p. 3895-903.
65. Klemm, R.W., et al., *Segregation of sphingolipids and sterols during formation of secretory vesicles at the trans-Golgi network*. J Cell Biol, 2009. **185**(4): p. 601-12.
66. Neukam, M., et al., *Purification of time-resolved insulin granules reveals proteomic and lipidomic changes during granule aging*. Cell Rep, 2024. **43**(3): p. 113836.
67. Holton, P., *The liberation of adenosine triphosphate on antidromic stimulation of sensory nerves*. J Physiol, 1959. **145**(3): p. 494-504.
68. Burnstock, G., *Purinergic nerves*. Pharmacol Rev, 1972. **24**(3): p. 509-81.
69. Khakh, B.S. and G. Burnstock, *The double life of ATP*. Sci Am, 2009. **301**(6): p. 84-90, 92.
70. Lazarowski, E.R., *Vesicular and conductive mechanisms of nucleotide release*. Purinergic Signal, 2012. **8**(3): p. 359-73.
71. Dahl, G. and R.W. Keane, *Pannexin: from discovery to bedside in 11±4 years?* Brain Res, 2012. **1487**: p. 150-9.
72. Moriyama, Y., et al., *Vesicular nucleotide transporter (VNUT): appearance of an actress on the stage of purinergic signaling*. Purinergic Signal, 2017. **13**(3): p. 387-404.
73. Ralevic, V. and G. Burnstock, *Receptors for purines and pyrimidines*. Pharmacol Rev, 1998. **50**(3): p. 413-92.
74. Grapengiesser, E., H. Dansk, and B. Hellman, *Pulses of external ATP aid to the synchronization of pancreatic beta-cells by generating premature Ca(2+) oscillations*. Biochem Pharmacol, 2004. **68**(4): p. 667-74.
75. Hellman, B., et al., *Cytoplasmic Ca<sup>2+</sup> oscillations in pancreatic beta-cells*. Biochim Biophys Acta, 1992. **1113**(3-4): p. 295-305.
76. Grapengiesser, E., E. Gylfe, and B. Hellman, *Synchronization of glucose-induced Ca<sup>2+</sup> transients in pancreatic beta-cells by a diffusible factor*. Biochem Biophys Res Commun, 1999. **254**(2): p. 436-9.
77. Aberer, W., et al., *A characterization of the nucleotide uptake of chromaffin granules of bovine adrenal medulla*. Biochem J, 1978. **172**(3): p. 353-60.
78. Bankston, L.A. and G. Guidotti, *Characterization of ATP transport into chromaffin granule ghosts. Synergy of ATP and serotonin accumulation in chromaffin granule ghosts*. J Biol Chem, 1996. **271**(29): p. 17132-8.

79. Reimer, R.J. and R.H. Edwards, *Organic anion transport is the primary function of the SLC17/type I phosphate transporter family*. Pflugers Arch, 2004. **447**(5): p. 629-35.
80. Sawada, K., et al., *Identification of a vesicular nucleotide transporter*. Proc Natl Acad Sci U S A, 2008. **105**(15): p. 5683-6.
81. Larsson, M., et al., *Functional and anatomical identification of a vesicular transporter mediating neuronal ATP release*. Cereb Cortex, 2012. **22**(5): p. 1203-14.
82. Jung, S.K., et al., *Transmembrane topology of vesicular glutamate transporter 2*. Biol Pharm Bull, 2006. **29**(3): p. 547-9.
83. Sakamoto, S., et al., *Impairment of vesicular ATP release affects glucose metabolism and increases insulin sensitivity*. Sci Rep, 2014. **4**: p. 6689.
84. Geisler, J.C., et al., *Vesicular Nucleotide Transporter-Mediated ATP Release Regulates Insulin Secretion*. Endocrinology, 2013. **154**(2): p. 675-684.
85. Dlasková, A., et al., *4Pi microscopy reveals an impaired three-dimensional mitochondrial network of pancreatic islet beta-cells, an experimental model of type-2 diabetes*. Biochim Biophys Acta, 2010. **1797**(6-7): p. 1327-41.
86. Chan, D.C., *Fusion and fission: interlinked processes critical for mitochondrial health*. Annu Rev Genet, 2012. **46**: p. 265-87.
87. Chan, D.C., *Mitochondria: dynamic organelles in disease, aging, and development*. Cell, 2006. **125**(7): p. 1241-52.
88. Yoon, Y., et al., *Mitochondrial dynamics in diabetes*. Antioxid Redox Signal, 2011. **14**(3): p. 439-57.
89. Newsholme, P., et al., *Diabetes associated cell stress and dysfunction: role of mitochondrial and non-mitochondrial ROS production and activity*. J Physiol, 2007. **583**(Pt 1): p. 9-24.
90. Erion, K.A., et al., *Chronic Exposure to Excess Nutrients Left-shifts the Concentration Dependence of Glucose-stimulated Insulin Secretion in Pancreatic  $\beta$ -Cells*. J Biol Chem, 2015. **290**(26): p. 16191-201.
91. Chang-Chen, K.J., R. Mullur, and E. Bernal-Mizrachi, *Beta-cell failure as a complication of diabetes*. Rev Endocr Metab Disord, 2008. **9**(4): p. 329-43.
92. Anello, M., et al., *Functional and morphological alterations of mitochondria in pancreatic beta cells from type 2 diabetic patients*. Diabetologia, 2005. **48**(2): p. 282-9.
93. Deng, S., et al., *Structural and functional abnormalities in the islets isolated from type 2 diabetic subjects*. Diabetes, 2004. **53**(3): p. 624-32.
94. Sidarala, V., et al., *Mitofusin 1 and 2 regulation of mitochondrial DNA content is a critical determinant of glucose homeostasis*. Nat Commun, 2022. **13**(1): p. 2340.
95. Mears, J.A., et al., *Conformational changes in Dnm1 support a contractile mechanism for mitochondrial fission*. Nat Struct Mol Biol, 2011. **18**(1): p. 20-6.
96. Jheng, H.F., et al., *Mitochondrial fission contributes to mitochondrial dysfunction and insulin resistance in skeletal muscle*. Mol Cell Biol, 2012. **32**(2): p. 309-19.
97. Hennings, T.G., et al., *In Vivo Deletion of  $\beta$ -Cell Drp1 Impairs Insulin Secretion Without Affecting Islet Oxygen Consumption*. Endocrinology, 2018. **159**(9): p. 3245-3256.
98. Kakihana, T., K. Nagata, and R. Sitia, *Peroxides and peroxidases in the endoplasmic reticulum: integrating redox homeostasis and oxidative folding*. Antioxid Redox Signal, 2012. **16**(8): p. 763-71.

99. Shai, N., et al., *Systematic mapping of contact sites reveals tethers and a function for the peroxisome-mitochondria contact*. Nat Commun, 2018. **9**(1): p. 1761.
100. Valm, A.M., et al., *Applying systems-level spectral imaging and analysis to reveal the organelle interactome*. Nature, 2017. **546**(7656): p. 162-167.
101. Fernández-Busnadiego, R., Y. Saheki, and P. De Camilli, *Three-dimensional architecture of extended synaptotagmin-mediated endoplasmic reticulum-plasma membrane contact sites*. Proc Natl Acad Sci U S A, 2015. **112**(16): p. E2004-13.
102. Dickson, E.J., *Endoplasmic Reticulum-Plasma Membrane Contacts Regulate Cellular Excitability*. Adv Exp Med Biol, 2017. **997**: p. 95-109.
103. Lewis, S.C., L.F. Uchiyama, and J. Nunnari, *ER-mitochondria contacts couple mtDNA synthesis with mitochondrial division in human cells*. Science, 2016. **353**(6296): p. aaf5549.
104. Friedman, J.R., et al., *ER tubules mark sites of mitochondrial division*. Science, 2011. **334**(6054): p. 358-62.
105. Wu, Y., et al., *Contacts between the endoplasmic reticulum and other membranes in neurons*. Proc Natl Acad Sci U S A, 2017. **114**(24): p. E4859-e4867.
106. Scorrano, L., et al., *BAX and BAK regulation of endoplasmic reticulum Ca<sup>2+</sup>: a control point for apoptosis*. Science, 2003. **300**(5616): p. 135-9.
107. Garofalo, T., et al., *Evidence for the involvement of lipid rafts localized at the ER-mitochondria associated membranes in autophagosome formation*. Autophagy, 2016. **12**(6): p. 917-35.
108. Poston, C.N., et al., *Proteomic analysis of lipid raft-enriched membranes isolated from internal organelles*. Biochem Biophys Res Commun, 2011. **415**(2): p. 355-60.
109. Wong, Y.C., W. Peng, and D. Krainc, *Lysosomal Regulation of Inter-mitochondrial Contact Fate and Motility in Charcot-Marie-Tooth Type 2*. Dev Cell, 2019. **50**(3): p. 339-354.e4.
110. Furuita, K., et al., *Electrostatic interaction between oxysterol-binding protein and VAMP-associated protein A revealed by NMR and mutagenesis studies*. J Biol Chem, 2010. **285**(17): p. 12961-70.
111. Kaiser, S.E., et al., *Structural basis of FFAT motif-mediated ER targeting*. Structure, 2005. **13**(7): p. 1035-45.
112. Loewen, C.J., A. Roy, and T.P. Levine, *A conserved ER targeting motif in three families of lipid binding proteins and in Opi1p binds VAP*. Embo j, 2003. **22**(9): p. 2025-35.
113. Wyles, J.P., C.R. McMaster, and N.D. Ridgway, *Vesicle-associated membrane protein-associated protein-A (VAP-A) interacts with the oxysterol-binding protein to modify export from the endoplasmic reticulum*. J Biol Chem, 2002. **277**(33): p. 29908-18.
114. Levine, T.P. and S. Munro, *Dual targeting of Osh1p, a yeast homologue of oxysterol-binding protein, to both the Golgi and the nucleus-vacuole junction*. Mol Biol Cell, 2001. **12**(6): p. 1633-44.
115. Ridgway, N.D., et al., *Translocation of oxysterol binding protein to Golgi apparatus triggered by ligand binding*. J Cell Biol, 1992. **116**(2): p. 307-19.
116. Mesmin, B., et al., *A four-step cycle driven by PI(4)P hydrolysis directs sterol/PI(4)P exchange by the ER-Golgi tether OSBP*. Cell, 2013. **155**(4): p. 830-43.
117. Lees, J.A., et al., *Lipid transport by TMEM24 at ER-plasma membrane contacts regulates pulsatile insulin secretion*. Science, 2017. **355**(6326).



118. Sun, E.W., et al., *Lipid transporter TMEM24/C2CD2L is a Ca(2+)-regulated component of ER-plasma membrane contacts in mammalian neurons*. Proc Natl Acad Sci U S A, 2019. **116**(12): p. 5775-5784.
119. Thivolet, C., et al., *Reduction of endoplasmic reticulum- mitochondria interactions in beta cells from patients with type 2 diabetes*. PLoS One, 2017. **12**(7): p. e0182027.
120. Dingreville, F., et al., *Differential Effect of Glucose on ER-Mitochondria Ca(2+) Exchange Participates in Insulin Secretion and Glucotoxicity-Mediated Dysfunction of  $\beta$ -Cells*. Diabetes, 2019. **68**(9): p. 1778-1794.
121. Tarasov, A.I., et al., *The mitochondrial Ca<sup>2+</sup> uniporter MCU is essential for glucose-induced ATP increases in pancreatic  $\beta$ -cells*. PLoS One, 2012. **7**(7): p. e39722.
122. Cárdenas, C., et al., *Essential regulation of cell bioenergetics by constitutive InsP3 receptor Ca<sup>2+</sup> transfer to mitochondria*. Cell, 2010. **142**(2): p. 270-83.
123. Gwiazda, K.S., et al., *Effects of palmitate on ER and cytosolic Ca<sup>2+</sup> homeostasis in beta-cells*. Am J Physiol Endocrinol Metab, 2009. **296**(4): p. E690-701.
124. Kono, T., et al., *Impaired Store-Operated Calcium Entry and STIM1 Loss Lead to Reduced Insulin Secretion and Increased Endoplasmic Reticulum Stress in the Diabetic  $\beta$ -Cell*. Diabetes, 2018. **67**(11): p. 2293-2304.
125. Petkovic, M., C.E. O'Brien, and Y.N. Jan, *Interorganelle communication, aging, and neurodegeneration*. Genes Dev, 2021. **35**(7-8): p. 449-469.
126. Herker, E., et al., *Lipid Droplet Contact Sites in Health and Disease*. Trends Cell Biol, 2021. **31**(5): p. 345-358.
127. Lim, C.Y., et al., *ER-lysosome contacts enable cholesterol sensing by mTORC1 and drive aberrant growth signalling in Niemann-Pick type C*. Nat Cell Biol, 2019. **21**(10): p. 1206-1218.
128. Hirabayashi, Y., et al., *ER-mitochondria tethering by PDZD8 regulates Ca(2+) dynamics in mammalian neurons*. Science, 2017. **358**(6363): p. 623-630.
129. Schon, E.A. and E. Area-Gomez, *Is Alzheimer's disease a disorder of mitochondria-associated membranes?* J Alzheimers Dis, 2010. **20 Suppl 2**: p. S281-92.
130. Stoica, R., et al., *ER-mitochondria associations are regulated by the VAPB-PTPIP51 interaction and are disrupted by ALS/FTD-associated TDP-43*. Nat Commun, 2014. **5**: p. 3996.
131. Cali, T., et al., *splitGFP Technology Reveals Dose-Dependent ER-Mitochondria Interface Modulation by  $\alpha$ -Synuclein A53T and A30P Mutants*. Cells, 2019. **8**(9).
132. Guardia-Laguarta, C., et al.,  *$\alpha$ -Synuclein is localized to mitochondria-associated ER membranes*. J Neurosci, 2014. **34**(1): p. 249-59.
133. Gautier, C.A., et al., *The endoplasmic reticulum-mitochondria interface is perturbed in PARK2 knockout mice and patients with PARK2 mutations*. Hum Mol Genet, 2016. **25**(14): p. 2972-2984.
134. Cali, T., et al.,  *$\alpha$ -Synuclein controls mitochondrial calcium homeostasis by enhancing endoplasmic reticulum-mitochondria interactions*. J Biol Chem, 2012. **287**(22): p. 17914-29.
135. Ottolini, D., et al., *The Parkinson disease-related protein DJ-1 counteracts mitochondrial impairment induced by the tumour suppressor protein p53 by enhancing endoplasmic reticulum-mitochondria tethering*. Hum Mol Genet, 2013. **22**(11): p. 2152-68.
136. McLelland, G.L., et al., *Mfn2 ubiquitination by PINK1/parkin gates the p97-dependent release of ER from mitochondria to drive mitophagy*. Elife, 2018. **7**.

137. Mitne-Neto, M., et al., *Downregulation of VAPB expression in motor neurons derived from induced pluripotent stem cells of ALS8 patients*. Hum Mol Genet, 2011. **20**(18): p. 3642-52.
138. Kim, S., et al., *Dysregulation of mitochondria-lysosome contacts by GBA1 dysfunction in dopaminergic neuronal models of Parkinson's disease*. Nat Commun, 2021. **12**(1): p. 1807.
139. Betz, C., et al., *Feature Article: mTOR complex 2-Akt signaling at mitochondria-associated endoplasmic reticulum membranes (MAM) regulates mitochondrial physiology*. Proc Natl Acad Sci U S A, 2013. **110**(31): p. 12526-34.
140. Fels, D.R. and C. Koumenis, *The PERK/eIF2alpha/ATF4 module of the UPR in hypoxia resistance and tumor growth*. Cancer Biol Ther, 2006. **5**(7): p. 723-8.
141. Bu, Y. and J.A. Diehl, *PERK Integrates Oncogenic Signaling and Cell Survival During Cancer Development*. J Cell Physiol, 2016. **231**(10): p. 2088-96.
142. Wadhwa, R., et al., *Upregulation of mortalin/mthsp70/Grp75 contributes to human carcinogenesis*. Int J Cancer, 2006. **118**(12): p. 2973-80.
143. Pernemalm, M., et al., *Quantitative proteomics profiling of primary lung adenocarcinoma tumors reveals functional perturbations in tumor metabolism*. J Proteome Res, 2013. **12**(9): p. 3934-43.
144. Shoshan-Barmatz, V., et al., *The mitochondrial voltage-dependent anion channel 1 in tumor cells*. Biochim Biophys Acta, 2015. **1848**(10 Pt B): p. 2547-75.
145. Giorgi, C., et al., *p53 at the endoplasmic reticulum regulates apoptosis in a Ca<sup>2+</sup>-dependent manner*. Proc Natl Acad Sci U S A, 2015. **112**(6): p. 1779-84.
146. Bononi, A., et al., *Identification of PTEN at the ER and MAMs and its regulation of Ca(2+) signaling and apoptosis in a protein phosphatase-dependent manner*. Cell Death Differ, 2013. **20**(12): p. 1631-43.
147. Giorgi, C., et al., *PML regulates apoptosis at endoplasmic reticulum by modulating calcium release*. Science, 2010. **330**(6008): p. 1247-51.
148. Missiroli, S., et al., *PML at Mitochondria-Associated Membranes Is Critical for the Repression of Autophagy and Cancer Development*. Cell Rep, 2016. **16**(9): p. 2415-27.
149. Butler, A.E., et al., *Beta-cell deficit and increased beta-cell apoptosis in humans with type 2 diabetes*. Diabetes, 2003. **52**(1): p. 102-10.
150. Rahier, J., et al., *Pancreatic beta-cell mass in European subjects with type 2 diabetes*. Diabetes Obes Metab, 2008. **10 Suppl 4**: p. 32-42.
151. Barlow, J. and C. Affourtit, *Novel insights into pancreatic  $\beta$ -cell glucolipototoxicity from real-time functional analysis of mitochondrial energy metabolism in INS-1E insulinoma cells*. Biochem J, 2013. **456**(3): p. 417-26.
152. Masini, M., et al., *Prevention by metformin of alterations induced by chronic exposure to high glucose in human islet beta cells is associated with preserved ATP/ADP ratio*. Diabetes Res Clin Pract, 2014. **104**(1): p. 163-70.
153. Madec, A.M., et al., *Role of mitochondria-associated endoplasmic reticulum membrane (MAMs) interactions and calcium exchange in the development of type 2 diabetes*. Int Rev Cell Mol Biol, 2021. **363**: p. 169-202.
154. Karunakaran, U., et al., *Guards and culprits in the endoplasmic reticulum: glucolipototoxicity and  $\beta$ -cell failure in type II diabetes*. Exp Diabetes Res, 2012. **2012**: p. 639762.
155. Theurey, P., et al., *Mitochondria-associated endoplasmic reticulum membranes allow adaptation of mitochondrial metabolism to glucose availability in the liver*. J Mol Cell Biol, 2016. **8**(2): p. 129-43.

156. Tubbs, E., et al., *Mitochondria-associated endoplasmic reticulum membrane (MAM) integrity is required for insulin signaling and is implicated in hepatic insulin resistance*. *Diabetes*, 2014. **63**(10): p. 3279-94.
157. Arruda, A.P., et al., *Chronic enrichment of hepatic endoplasmic reticulum-mitochondria contact leads to mitochondrial dysfunction in obesity*. *Nat Med*, 2014. **20**(12): p. 1427-35.
158. Behnia, R. and S. Munro, *Organelle identity and the signposts for membrane traffic*. *Nature*, 2005. **438**(7068): p. 597-604.
159. Balla, T., *Phosphoinositides: tiny lipids with giant impact on cell regulation*. *Physiol Rev*, 2013. **93**(3): p. 1019-137.
160. Bilanges, B., Y. Posor, and B. Vanhaesebroeck, *PI3K isoforms in cell signalling and vesicle trafficking*. *Nat Rev Mol Cell Biol*, 2019. **20**(9): p. 515-534.
161. Di Paolo, G. and P. De Camilli, *Phosphoinositides in cell regulation and membrane dynamics*. *Nature*, 2006. **443**(7112): p. 651-7.
162. Posor, Y., W. Jang, and V. Haucke, *Phosphoinositides as membrane organizers*. *Nat Rev Mol Cell Biol*, 2022. **23**(12): p. 797-816.
163. Godi, A., et al., *ARF mediates recruitment of PtdIns-4-OH kinase-beta and stimulates synthesis of PtdIns(4,5)P2 on the Golgi complex*. *Nat Cell Biol*, 1999. **1**(5): p. 280-7.
164. Sasaki, J., et al., *ACBD3-mediated recruitment of PI4KB to picornavirus RNA replication sites*. *Embo j*, 2012. **31**(3): p. 754-66.
165. Szentpetery, Z., P. Várnai, and T. Balla, *Acute manipulation of Golgi phosphoinositides to assess their importance in cellular trafficking and signaling*. *Proc Natl Acad Sci U S A*, 2010. **107**(18): p. 8225-30.
166. Wang, Y.J., et al., *Phosphatidylinositol 4 phosphate regulates targeting of clathrin adaptor AP-1 complexes to the Golgi*. *Cell*, 2003. **114**(3): p. 299-310.
167. Rahajeng, J., et al., *Efficient Golgi Forward Trafficking Requires GOLPH3-Driven, PI4P-Dependent Membrane Curvature*. *Dev Cell*, 2019. **50**(5): p. 573-585.e5.
168. De Matteis, M.A. and A. Luini, *Exiting the Golgi complex*. *Nat Rev Mol Cell Biol*, 2008. **9**(4): p. 273-84.
169. Mahajan, D., et al., *Dopey1-Mon2 complex binds to dual-lipids and recruits kinesin-1 for membrane trafficking*. *Nat Commun*, 2019. **10**(1): p. 3218.
170. Valente, C., et al., *A 14-3-3γ dimer-based scaffold bridges CtBP1-S/BARS to PI(4)KIIIβ to regulate post-Golgi carrier formation*. *Nat Cell Biol*, 2012. **14**(4): p. 343-54.
171. Liljedahl, M., et al., *Protein kinase D regulates the fission of cell surface destined transport carriers from the trans-Golgi network*. *Cell*, 2001. **104**(3): p. 409-20.
172. Baron, C.L. and V. Malhotra, *Role of diacylglycerol in PKD recruitment to the TGN and protein transport to the plasma membrane*. *Science*, 2002. **295**(5553): p. 325-8.
173. Hausser, A., et al., *Protein kinase D regulates vesicular transport by phosphorylating and activating phosphatidylinositol-4 kinase IIIbeta at the Golgi complex*. *Nat Cell Biol*, 2005. **7**(9): p. 880-6.
174. Lu, D., et al., *Phosphatidylinositol 4-kinase IIa is palmitoylated by Golgi-localized palmitoyltransferases in cholesterol-dependent manner*. *J Biol Chem*, 2012. **287**(26): p. 21856-65.
175. Blagoveshchenskaya, A., et al., *Integration of Golgi trafficking and growth factor signaling by the lipid phosphatase SAC1*. *J Cell Biol*, 2008. **180**(4): p. 803-12.

176. Shin, J.J.H., et al., *pH Biosensing by PI4P Regulates Cargo Sorting at the TGN*. *Dev Cell*, 2020. **52**(4): p. 461-476.e4.
177. Hammond, G.R., et al., *PI4P and PI(4,5)P2 are essential but independent lipid determinants of membrane identity*. *Science*, 2012. **337**(6095): p. 727-30.
178. Sohn, M., et al., *PI(4,5)P(2) controls plasma membrane PI4P and PS levels via ORP5/8 recruitment to ER-PM contact sites*. *J Cell Biol*, 2018. **217**(5): p. 1797-1813.
179. Prinz, W.A., A. Toulmay, and T. Balla, *The functional universe of membrane contact sites*. *Nature Reviews Molecular Cell Biology*, 2020. **21**(1): p. 7-24.
180. Shirane, M., et al., *Protrudin and PDZD8 contribute to neuronal integrity by promoting lipid extraction required for endosome maturation*. *Nat Commun*, 2020. **11**(1): p. 4576.
181. Bakula, D., et al., *WIPI3 and WIPI4  $\beta$ -propellers are scaffolds for LKB1-AMPK-TSC signalling circuits in the control of autophagy*. *Nat Commun*, 2017. **8**: p. 15637.
182. Churchward, M.A. and J.R. Coorssen, *Cholesterol, regulated exocytosis and the physiological fusion machine*. *Biochem J*, 2009. **423**(1): p. 1-14.
183. Gondré-Lewis, M.C., et al., *Abnormal sterols in cholesterol-deficiency diseases cause secretory granule malformation and decreased membrane curvature*. *J Cell Sci*, 2006. **119**(Pt 9): p. 1876-85.
184. Acton, S., et al., *Identification of scavenger receptor SR-BI as a high density lipoprotein receptor*. *Science*, 1996. **271**(5248): p. 518-20.
185. Phillips, M.C., *Apolipoprotein E isoforms and lipoprotein metabolism*. *IUBMB Life*, 2014. **66**(9): p. 616-23.
186. Perego, C., et al., *Cholesterol metabolism, pancreatic  $\beta$ -cell function and diabetes*. *Biochim Biophys Acta Mol Basis Dis*, 2019. **1865**(9): p. 2149-2156.
187. Ishikawa, M., et al., *Cholesterol accumulation and diabetes in pancreatic beta-cell-specific SREBP-2 transgenic mice: a new model for lipotoxicity*. *J Lipid Res*, 2008. **49**(12): p. 2524-34.
188. Fryirs, M., P.J. Barter, and K.A. Rye, *Cholesterol metabolism and pancreatic beta-cell function*. *Curr Opin Lipidol*, 2009. **20**(3): p. 159-64.
189. van Meer, G., D.R. Voelker, and G.W. Feigenson, *Membrane lipids: where they are and how they behave*. *Nat Rev Mol Cell Biol*, 2008. **9**(2): p. 112-24.
190. Ikonen, E., *Cellular cholesterol trafficking and compartmentalization*. *Nat Rev Mol Cell Biol*, 2008. **9**(2): p. 125-38.
191. Cnop, M., et al., *Low density lipoprotein can cause death of islet beta-cells by its cellular uptake and oxidative modification*. *Endocrinology*, 2002. **143**(9): p. 3449-53.
192. Lu, X., et al., *Cholesterol induces pancreatic  $\beta$  cell apoptosis through oxidative stress pathway*. *Cell Stress Chaperones*, 2011. **16**(5): p. 539-48.
193. Bogan, J.S., Y. Xu, and M. Hao, *Cholesterol accumulation increases insulin granule size and impairs membrane trafficking*. *Traffic*, 2012. **13**(11): p. 1466-80.
194. Hussain, S.S., et al., *Control of insulin granule formation and function by the ABC transporters ABCG1 and ABCA1 and by oxysterol binding protein OSBP*. *Mol Biol Cell*, 2018. **29**(10): p. 1238-1257.
195. Salaün, C., D.J. James, and L.H. Chamberlain, *Lipid rafts and the regulation of exocytosis*. *Traffic*, 2004. **5**(4): p. 255-64.
196. Skelin, M., M. Rupnik, and A. Cencic, *Pancreatic beta cell lines and their applications in diabetes mellitus research*. *Altex*, 2010. **27**(2): p. 105-13.

197. Miyazaki, J., et al., *Establishment of a pancreatic beta cell line that retains glucose-inducible insulin secretion: special reference to expression of glucose transporter isoforms*. *Endocrinology*, 1990. **127**(1): p. 126-32.
198. Brenner, M.B. and H.J. Mest, *A buffer temperature controlled perfusion system to study temperature dependence and kinetics of insulin secretion in MIN6 pseudoislets*. *J Pharmacol Toxicol Methods*, 2004. **50**(1): p. 53-7.
199. Hauge-Evans, A.C., et al., *Role of adenine nucleotides in insulin secretion from MIN6 pseudoislets*. *Mol Cell Endocrinol*, 2002. **191**(2): p. 167-76.
200. Hauge-Evans, A.C., et al., *Pancreatic beta-cell-to-beta-cell interactions are required for integrated responses to nutrient stimuli: enhanced  $Ca^{2+}$  and insulin secretory responses of MIN6 pseudoislets*. *Diabetes*, 1999. **48**(7): p. 1402-8.
201. Kelly, C., et al., *Comparison of insulin release from MIN6 pseudoislets and pancreatic islets of Langerhans reveals importance of homotypic cell interactions*. *Pancreas*, 2010. **39**(7): p. 1016-23.
202. Rogers, G.J., M.N. Hodgkin, and P.E. Squires, *E-cadherin and cell adhesion: a role in architecture and function in the pancreatic islet*. *Cell Physiol Biochem*, 2007. **20**(6): p. 987-94.
203. Chowdhury, A., et al., *Functional differences between aggregated and dispersed insulin-producing cells*. *Diabetologia*, 2013. **56**(7): p. 1557-68.
204. Meda, P., et al., *In vivo modulation of connexin 43 gene expression and junctional coupling of pancreatic B-cells*. *Exp Cell Res*, 1991. **192**(2): p. 469-80.
205. Yu, Q., et al., *Glucose controls glucagon secretion by directly modulating cAMP in alpha cells*. *Diabetologia*, 2019. **62**(7): p. 1212-1224.
206. Ettinger, A. and T. Wittmann, *Fluorescence live cell imaging*. *Methods Cell Biol*, 2014. **123**: p. 77-94.
207. Icha, J., et al., *Phototoxicity in live fluorescence microscopy, and how to avoid it*. *Bioessays*, 2017. **39**(8).
208. Steyer, J.A. and W. Almers, *A real-time view of life within 100 nm of the plasma membrane*. *Nat Rev Mol Cell Biol*, 2001. **2**(4): p. 268-75.
209. Berridge, M.J., *Inositol trisphosphate and calcium signalling*. *Nature*, 1993. **361**(6410): p. 315-25.
210. Floto, R.A., et al., *IgG-induced  $Ca^{2+}$  oscillations in differentiated U937 cells; a study using laser scanning confocal microscopy and co-loaded fluo-3 and fura-red fluorescent probes*. *Cell Calcium*, 1995. **18**(5): p. 377-89.
211. Lipp, P. and E. Niggli, *Ratiometric confocal  $Ca(2+)$ -measurements with visible wavelength indicators in isolated cardiac myocytes*. *Cell Calcium*, 1993. **14**(5): p. 359-72.
212. Nicotera, P. and A.D. Rossi, *Nuclear  $Ca^{2+}$ : physiological regulation and role in apoptosis*. *Mol Cell Biochem*, 1994. **135**(1): p. 89-98.
213. Schild, D., A. Jung, and H.A. Schultens, *Localization of calcium entry through calcium channels in olfactory receptor neurones using a laser scanning microscope and the calcium indicator dyes Fluo-3 and Fura-Red*. *Cell Calcium*, 1994. **15**(5): p. 341-8.
214. Takahashi, A., et al., *Measurement of intracellular calcium*. *Physiol Rev*, 1999. **79**(4): p. 1089-125.
215. Palmer, A.E. and R.Y. Tsien, *Measuring calcium signaling using genetically targetable fluorescent indicators*. *Nat Protoc*, 2006. **1**(3): p. 1057-65.
216. Rehberg, M., et al., *A new non-disruptive strategy to target calcium indicator dyes to the endoplasmic reticulum*. *Cell Calcium*, 2008. **44**(4): p. 386-99.
217. Paredes, R.M., et al., *Chemical calcium indicators*. *Methods*, 2008. **46**(3): p. 143-51.

218. Heckman, C.A., O.M. Ademuyiwa, and M.L. Cayer, *How filopodia respond to calcium in the absence of a calcium-binding structural protein: non-channel functions of TRP*. Cell Commun Signal, 2022. **20**(1): p. 130.
219. Kao, J.P. and R.Y. Tsien, *Ca<sup>2+</sup> binding kinetics of fura-2 and azo-1 from temperature-jump relaxation measurements*. Biophys J, 1988. **53**(4): p. 635-9.
220. Miyawaki, A., et al., *Fluorescent indicators for Ca<sup>2+</sup> based on green fluorescent proteins and calmodulin*. Nature, 1997. **388**(6645): p. 882-7.
221. Nakai, J., M. Ohkura, and K. Imoto, *A high signal-to-noise Ca(2+) probe composed of a single green fluorescent protein*. Nat Biotechnol, 2001. **19**(2): p. 137-41.
222. Zhao, Y., et al., *An expanded palette of genetically encoded Ca<sup>2+</sup> indicators*. Science, 2011. **333**(6051): p. 1888-91.
223. Greotti, E., et al., *Characterization of the ER-Targeted Low Affinity Ca(2+) Probe D4ER*. Sensors (Basel), 2016. **16**(9).
224. Bernhard, W. and C. Rouiller, *Close topographical relationship between mitochondria and ergastoplasm of liver cells in a definite phase of cellular activity*. J Biophys Biochem Cytol, 1956. **2**(4 Suppl): p. 73-8.
225. Missiroli, S., et al., *Mitochondria-associated membranes (MAMs) and inflammation*. Cell Death Dis, 2018. **9**(3): p. 329.
226. Giorgi, C., et al., *Mitochondria-associated membranes: composition, molecular mechanisms, and physiopathological implications*. Antioxid Redox Signal, 2015. **22**(12): p. 995-1019.
227. Sala-Vila, A., et al., *Interplay between hepatic mitochondria-associated membranes, lipid metabolism and caveolin-1 in mice*. Sci Rep, 2016. **6**: p. 27351.
228. Csordás, G., et al., *Imaging interorganelle contacts and local calcium dynamics at the ER-mitochondrial interface*. Mol Cell, 2010. **39**(1): p. 121-32.
229. Drobne, D., *3D imaging of cells and tissues by focused ion beam/scanning electron microscopy (FIB/SEM)*. Methods Mol Biol, 2013. **950**: p. 275-92.
230. Fredriksson, S., et al., *Protein detection using proximity-dependent DNA ligation assays*. Nat Biotechnol, 2002. **20**(5): p. 473-7.
231. Benhammouda, S., et al., *Mitochondria Endoplasmic Reticulum Contact Sites (MERCs): Proximity Ligation Assay as a Tool to Study Organelle Interaction*. Front Cell Dev Biol, 2021. **9**: p. 789959.
232. Förster, T., *Zwischenmolekulare energiewanderung und fluoreszenz*. Annalen der physik, 1948. **437**(1-2): p. 55-75.
233. Alford, S.C., et al., *Dimerization-dependent green and yellow fluorescent proteins*. ACS Synth Biol, 2012. **1**(12): p. 569-75.
234. Tchekanda, E., D. Sivanesan, and S.W. Michnick, *An infrared reporter to detect spatiotemporal dynamics of protein-protein interactions*. Nat Methods, 2014. **11**(6): p. 641-4.
235. Subczynski, W.K., et al., *High Cholesterol/Low Cholesterol: Effects in Biological Membranes: A Review*. Cell Biochem Biophys, 2017. **75**(3-4): p. 369-385.
236. Ridsdale, A., et al., *Cholesterol is required for efficient endoplasmic reticulum-to-Golgi transport of secretory membrane proteins*. Mol Biol Cell, 2006. **17**(4): p. 1593-605.
237. Solanko, L.M., et al., *Membrane orientation and lateral diffusion of BODIPY-cholesterol as a function of probe structure*. Biophys J, 2013. **105**(9): p. 2082-92.
238. Waugh, C.M., et al., *Mild hypercholesterolemia impacts achilles sub-tendon mechanical properties in young rats*. BMC Musculoskelet Disord, 2023. **24**(1): p. 282.

239. Xie, B., et al., *Plasma Membrane Phosphatidylinositol 4,5-Bisphosphate Regulates Ca<sup>2+</sup>-Influx and Insulin Secretion from Pancreatic  $\beta$  Cells*. *Cell Chem Biol*, 2016. **23**(7): p. 816-826.
240. Lin, C.W., et al., *Membrane phosphoinositides control insulin secretion through their effects on ATP-sensitive K<sup>+</sup> channel activity*. *Diabetes*, 2005. **54**(10): p. 2852-2858.
241. Trexler, A.J. and J.W. Taraska, *Regulation of insulin exocytosis by calcium-dependent protein kinase C in beta cells*. *Cell Calcium*, 2017. **67**: p. 1-10.
242. Wuttke, A., *Lipid signalling dynamics at the  $\beta$ -cell plasma membrane*. *Basic Clin Pharmacol Toxicol*, 2015. **116**(4): p. 281-90.
243. Wuttke, A., O. Idevall-Hagren, and A. Tengholm, *P2Y<sub>1</sub> receptor-dependent diacylglycerol signaling microdomains in  $\beta$  cells promote insulin secretion*. *Faseb j*, 2013. **27**(4): p. 1610-20.
244. Wuttke, A., Q. Yu, and A. Tengholm, *Autocrine Signaling Underlies Fast Repetitive Plasma Membrane Translocation of Conventional and Novel Protein Kinase C Isoforms in  $\beta$  Cells*. *J Biol Chem*, 2016. **291**(29): p. 14986-95.
245. Pottkat, A., et al., *Insulin biosynthetic interaction network component, TMEM24, facilitates insulin reserve pool release*. *Cell Rep*, 2013. **4**(5): p. 921-30.
246. Xie, B., P.M. Nguyen, and O. Idevall-Hagren, *Feedback regulation of insulin secretion by extended synaptotagmin-1*. *Faseb j*, 2019. **33**(4): p. 4716-4728.
247. Roe, M.W., et al., *Thapsigargin inhibits the glucose-induced decrease of intracellular Ca<sup>2+</sup> in mouse islets of Langerhans*. *Am J Physiol*, 1994. **266**(6 Pt 1): p. E852-62.
248. Rosivatz, E. and R. Woscholski, *Removal or masking of phosphatidylinositol (4,5)bisphosphate from the outer mitochondrial membrane causes mitochondrial fragmentation*. *Cell Signal*, 2011. **23**(2): p. 478-86.
249. MacDonald, M.J., et al., *Characterization of phospholipids in insulin secretory granules and mitochondria in pancreatic beta cells and their changes with glucose stimulation*. *J Biol Chem*, 2015. **290**(17): p. 11075-92.
250. Cruz-Garcia, D., et al., *Recruitment of arfaptins to the trans-Golgi network by PI(4)P and their involvement in cargo export*. *Embo j*, 2013. **32**(12): p. 1717-29.
251. De Matteis, M.A., C. Wilson, and G. D'Angelo, *Phosphatidylinositol-4-phosphate: the Golgi and beyond*. *Bioessays*, 2013. **35**(7): p. 612-22.
252. Santiago-Tirado, F.H. and A. Bretscher, *Membrane-trafficking sorting hubs: cooperation between PI4P and small GTPases at the trans-Golgi network*. *Trends Cell Biol*, 2011. **21**(9): p. 515-25.
253. Nguyen, P.M., et al., *The PI(4)P phosphatase Sac2 controls insulin granule docking and release*. *J Cell Biol*, 2019. **218**(11): p. 3714-3729.
254. Levanon, D., et al., *cDNA cloning of human oxysterol-binding protein and localization of the gene to human chromosome 11 and mouse chromosome 19*. *Genomics*, 1990. **7**(1): p. 65-74.
255. Balla, A., et al., *Maintenance of hormone-sensitive phosphoinositide pools in the plasma membrane requires phosphatidylinositol 4-kinase III $\alpha$* . *Mol Biol Cell*, 2008. **19**(2): p. 711-21.
256. Malek, M., et al., *PTEN Regulates PI(3,4)P(2) Signaling Downstream of Class I PI3K*. *Mol Cell*, 2017. **68**(3): p. 566-580.e10.
257. Hao, M., et al., *Direct effect of cholesterol on insulin secretion: a novel mechanism for pancreatic beta-cell dysfunction*. *Diabetes*, 2007. **56**(9): p. 2328-38.
258. Cao, M., et al., *Absence of Sac2/INPP5F enhances the phenotype of a Parkinson's disease mutation of synaptotagmin I*. *Proc Natl Acad Sci U S A*, 2020. **117**(22): p. 12428-12434.

259. Jain, S. and K.A. Jacobson, *Purinergic signaling in diabetes and metabolism*. *Biochem Pharmacol*, 2021. **187**: p. 114393.
260. Boyer, C.K., et al., *Synchronized proinsulin trafficking reveals delayed Golgi export accompanies  $\beta$ -cell secretory dysfunction in rodent models of hyperglycemia*. *Sci Rep*, 2023. **13**(1): p. 5218.
261. Boncompain, G., et al., *Synchronization of secretory protein traffic in populations of cells*. *Nature Methods*, 2012. **9**(5): p. 493-498.
262. Daniele, T., et al., *Mitochondria and melanosomes establish physical contacts modulated by Mfn2 and involved in organelle biogenesis*. *Curr Biol*, 2014. **24**(4): p. 393-403.
263. Demarquoy, J. and F. Le Borgne, *Crosstalk between mitochondria and peroxisomes*. *World J Biol Chem*, 2015. **6**(4): p. 301-9.
264. Rieusset, J., *The role of endoplasmic reticulum-mitochondria contact sites in the control of glucose homeostasis: an update*. *Cell Death Dis*, 2018. **9**(3): p. 388.
265. Henquin, J.C., *Triggering and amplifying pathways of regulation of insulin secretion by glucose*. *Diabetes*, 2000. **49**(11): p. 1751-60.
266. Idevall-Hagren, O., et al., *cAMP mediators of pulsatile insulin secretion from glucose-stimulated single beta-cells*. *J Biol Chem*, 2010. **285**(30): p. 23007-18.
267. Lam, S.S., et al., *Directed evolution of APEX2 for electron microscopy and proximity labeling*. *Nat Methods*, 2015. **12**(1): p. 51-4.
268. Rhee, H.W., et al., *Proteomic mapping of mitochondria in living cells via spatially restricted enzymatic tagging*. *Science*, 2013. **339**(6125): p. 1328-1331.
269. Roux, K.J., et al., *A promiscuous biotin ligase fusion protein identifies proximal and interacting proteins in mammalian cells*. *J Cell Biol*, 2012. **196**(6): p. 801-10.
270. Branon, T.C., et al., *Efficient proximity labeling in living cells and organisms with TurboID*. *Nat Biotechnol*, 2018. **36**(9): p. 880-887.
271. Han, Y., et al., *Directed Evolution of Split APEX2 Peroxidase*. *ACS Chem Biol*, 2019. **14**(4): p. 619-635.
272. De Munter, S., et al., *Split-BioID: a proximity biotinylation assay for dimerization-dependent protein interactions*. *FEBS Lett*, 2017. **591**(2): p. 415-424.
273. Kwak, C., et al., *Contact-ID, a tool for profiling organelle contact sites, reveals regulatory proteins of mitochondrial-associated membrane formation*. *Proc Natl Acad Sci U S A*, 2020. **117**(22): p. 12109-12120.
274. Schopp, I.M., et al., *Split-BioID a conditional proteomics approach to monitor the composition of spatiotemporally defined protein complexes*. *Nat Commun*, 2017. **8**: p. 15690.
275. Lee, J. and U. Ozcan, *Unfolded protein response signaling and metabolic diseases*. *J Biol Chem*, 2014. **289**(3): p. 1203-11.
276. Shrestha, N., et al., *Pathological  $\beta$ -Cell Endoplasmic Reticulum Stress in Type 2 Diabetes: Current Evidence*. *Front Endocrinol (Lausanne)*, 2021. **12**: p. 650158.
277. Yong, J., et al., *Therapeutic opportunities for pancreatic  $\beta$ -cell ER stress in diabetes mellitus*. *Nat Rev Endocrinol*, 2021. **17**(8): p. 455-467.
278. Zhang, X., et al., *Visualizing insulin vesicle neighborhoods in  $\beta$  cells by cryo-electron tomography*. *Sci Adv*, 2020. **6**(50).





# Acta Universitatis Upsaliensis

*Digital Comprehensive Summaries of Uppsala Dissertations from the Faculty of Medicine 2114*

Editor: The Dean of the Faculty of Medicine

A doctoral dissertation from the Faculty of Medicine, Uppsala University, is usually a summary of a number of papers. A few copies of the complete dissertation are kept at major Swedish research libraries, while the summary alone is distributed internationally through the series Digital Comprehensive Summaries of Uppsala Dissertations from the Faculty of Medicine. (Prior to January, 2005, the series was published under the title “Comprehensive Summaries of Uppsala Dissertations from the Faculty of Medicine”.)

Distribution: [publications.uu.se](http://publications.uu.se)  
urn:nbn:se:uu:diva-544607



ACTA UNIVERSITATIS  
UPSALIENSIS  
2025